EXPERIMENTAL STUDY OF EXTERNALLY FLANGE BONDED CFRP FOR RETROFITTING BEAM-COLUMN JOINTS WITH HIGH CONCRETE COMPRESSIVE STRENGTH UNDER CYCLIC LOADING

BY

OLANIYI SOLOMON AROWOJOLU

A Thesis Presented to the
DEANSHIP OF GRADUATE STUDIES

KING FAHD UNIVERSITY OF PETROLEUM & MINERALS

DHAHRAN, SAUDI ARABIA

In Partial Fulfillment of the
Requirements for the Degree of

MASTER OF SCIENCE

In

CIVIL ENGINEERING

NOVEMBER, 2016.

KING FAHD UNIVERSITY OF PETROLEUM & MINERALS

DHAHRAN- 31261, SAUDI ARABIA

DEANSHIP OF GRADUATE STUDIES

This thesis, written by **OLANIYI SOLOMON AROWOJOLU** under the direction his thesis advisor and approved by his thesis committee, has been presented and accepted by the Dean of Graduate Studies, in partial fulfillment of the requirements for the degree of **MASTER OF SCIENCE IN CIVIL ENGINEERING.**

Dr. Ali Al-Gadhib
(Advisor)

Dr. Salah U. Al-Dulaijan
Department Chairman

Dr. Muhammad K. Rahman
(Co-Advisor)

Dr. Salam A. Zummo
Dean of Graduate Studies

Dr. Mohammed Al-Osta
(Member)

30/11/16
Date

Dr. Husain J. Al-Gahtani
(Member)

Dr. Alfarabi M. Sharif
(Member)

This work is dedicated to GOD Almighty, the giver of wisdom and strength.

ACKNOWLEDGMENTS

My profound gratitude goes to the Almighty God, who knows the end of a journey right from the beginning. This journey could not have been possible without HIM. It is HIS grace that has made it possible for me to begin this journey and complete it successfully. To HIM alone be all the praises.

The financial support plus a conducive learning environment provided by the ministry of higher education through the King Fahd University of Petroleum and Minerals, Dhahran, Saudi Arabia during my program is highly appreciated. I would also like to specially thank the Center for Engineering Research for providing rare opportunities that made my studies easier than anticipated. The support received from Prainsa Precast Concrete Factory and Saudi SIKA for the provision of the CFRP and epoxy used for this research is much appreciated.

I will like to say a big thank you to my advisor Dr. Ali Al-Gadhib for his supports and assistance during my course of study. My appreciation goes to my thesis co-advisor, Dr. Muhammad Kalimur Rahman, who stood by me throughout my study in KFUPM, with his patience, selfless effort, and personal effort in making sure that my opinion counts. His encouragement made research appealing and interested to me. Words are not enough to appreciate the support I received from Dr. Mohammed H. Baluch. He opened my eyes to opportunities that abound in every challenges. His contributions gave this research a meaning. I would like also to extend my gratitude to Dr. Mohammed Al-Osta for his brotherly advice, patience and contributions to this research. I am also grateful to Dr. Husain J. Gahtani and Dr. Alfarabi Sharif for their contributions during this research.

Special thanks to all the faculty members with whom I have taken courses. And to the lab technicians, I say thank you. Thanks also to Mr. Hurri and Dr. Ajmal for making the samples ready.

To all my friends who stood by me during this research, I am indeed grateful. I cannot but mention the assistance I received from Johnson Audu, Olakunle Francis Ojo, and Abu-Bakr Musa during the experimental work. To my Bahraini brother Ahmed Alali, I say a big thank you. I appreciate the support of my friends back home Falola Oluwafemi Paul, Dolapo Aiyegoro, and Kazeem Olumide Adelekan. To that special friend and sister-Olabisi Oshinaike who has made the biggest sacrifice for me to pursue this degree, I am indeed grateful, you mean so much to me dear.

Words are not enough to say thank for the support, sacrifice and efforts of Mr. and Mrs. Oladipo for standing by me all through thick and thin. I say a big thank you to my fellow teachers and students in the church and Engr. Ike Chukwuneke for having to cope without me during my program. I am indeed grateful to Mr. and Mrs. Omokaro for their supports and making my stay in Saudi Arabia a worthwhile. To the Nigerian community in the KFUPM, I say thank you.

This journey was made possible with the love, sacrifice, and unflinching supports of my parents, brother and sisters right from birth up till now. I am grateful. Finally, all glory belongs to HIM who alone stretched the heavens without structural supports.

TABLE OF CONTENTS

LIST OF TABLES

LIST OF FIGURES

LIST OF ABBREVIATIONS

AFRP: Aramid Fiber Reinforced Polymers

ALR: Axial Load Ratio

BCJ: Beam-Column Joint

BCJF: Beam-Column Joint Failure

BJF: Beam-Joint Failure

CAL: Column Axial Load

CFRP: Carbon Fiber Reinforced Polymer

CJF: Column Joint Failure

GFRP: Glass Fiber Reinforced Polymers

JF: Joint Failure

SMA: Shape Memory Alloy

UHPC: Ultra-High Performance Concrete

ABSTRACT

Full Name : [Olaniyi Solomon Arowojolu]

Thesis Title : [Experimental Study of Externally Flange Bonded CFRP for Retrofitting Beam – Column Joints with high Concrete Compressive Strength Under Cyclic Loading]

Major Field : [Civil Engineering]

Date of Degree : [November, 2016]

Reinforced concrete buildings with moment resisting frames comprising of beam-column joints (BCJ), designed prior to introduction of seismic codes, are deficient when subjected to seismic loading. The weakest link in these structural framing is the BCJ. The BCJ can fail in shear during seismic event, resulting in irreparable damage to the building and possibly a collapse.

Several strategies for shear strengthening deficient joints in old buildings have been investigated and implemented in buildings over the past three decades using CFRP sheets and laminates. The shear failure in joints is successfully precluded, with the failure mode shifting to flexural hinging at the interface of the BCJ. A localized failure in the connecting beams away from the BCJ interface is a preferable failure mode rather than a plastic hinge formation at the interface.

In modern BCJ with high strength concrete having transverse reinforcement in joints, also failed by flexural hinging at the BCJ interface due to yielding of top reinforcement of the beam, which is again undesirable. This is undesirable because of yield penetration into the joint that may also lead to shear failure. It is therefore appropriate that all BCJ should

undergo a flexural failure with the plastic hinge formation away from the BCJ interface, well into in the connecting beam.

In this study, eight corner-external BCJ specimens of 1/3rd scale of a typical moment resisting frame, made with high strength concrete without transverse reinforcement were tested for monotonic and reversed cyclic test under displacement controlled regime. Four of these specimens were retrofitted with flange bonded unidirectional CFRP of different layers and different length. the specimen tested experimentally were also simulated in a commercially available finite element software- ABAQUS, using concrete damage plasticity and Tsai-Wu failure criteria for the CFRP-epoxy behavior.

In the experimental testing, the control specimens failed in flexure with formation of plastic hinge at the BCJ interface. The retrofitted specimen also failed by flexure but with the formation of the plastic hinge at the curtailment end of the CFRP. The relocation of the plastic hinge results in higher load capacity, improved ductility and energy dissipation of the specimens. The nonlinear finite element simulation shows similar results as observed in the experimental investigations. The experimental and numerical results were validated with analytical procedure using ACI 440 equations, by comparing the maximum loads, strains in the steel reinforcements and CFRP.

The approach retrofitting scheme presented is suitable for existing building, it is still of necessity to investigate how to design BCJ of moment resisting frame such that plastic hinge is formed inside the connecting beam for a new building.

ملخص الرسالة

الاسم الكامل: أولانيي سليمان أروجولو

عنوان الرسالة: : دراسة معملية لشفة CFRP مرتبطة خارجيا لإعادة تأهيل وصلات الأبيام-الاعمدة مكونة من الخرسانة ذات المقاومة العالية للضغط تحت تاثر الاحمال الترددية

التخصص: الهندسة المدنية

تاريخ الدرجة العلمية: نوفمبر 2016

المنشات الخرسانية المسلحة ذات الاطارات المقاومة للعزوم تتألف من وصلات الابيام -الأعمدة (beam-column joints)، قبل إستخدام المواصفات الزلزالية فإن عملية التصميم غير كافية عندما تتعرض هذه المنشات الى أحمال زلزالية. أضعف الوصلات في هذا النوع من الاطارات هي وصلات الابيام-الاعمدة. هذه الوصلات يمكن أن تفشل نتيجة للقص عند تعرضها لزلزال، مما ينتج عنه أضرار بالمبنى غير قابلة للمعالجة مع إحتمال انهيار المبنى.

عدة طرق لتدعيم القص في الوصلات الضعيفة في المباني القديمة قد تمت دراستها و تنفيذها على مباني في الثلاث عقودة الماضية باستخدام شرائح و صفائح CFRP. وجد أن الفشل الناتج من القص يمكن أن يمنع بنجاح بتحويل نوع الفشل إلى انعطاف مفصلي عند مناطق التلاقي في وصلات الابيام-الأعمدة. الفشل الموضعي في الابيام المتصلة بعيدا عن تداخل وصلات الابيام-الأعمدة هو المفضل دائما أكثر من تكون المفلصة اللدنة عند منطقة التداخل.

في وصلات الابيام-الأعمدة الحديثة المكونة من خرسانة عالية المقاومة و تسليح عرضي، فإن الفشل يحدث أيضا نتيجة للإنعطاف المفصلي عند منطقة تداخل الابيام-الاعمدة نتيجة لخضوع التسليح العلوي في البيم. و هذا أيضا غير مرغوب فيه لأن الخضوع يمكنه أن يتغلغل داخل الوصلة مما قد يؤدي أيضا إلى فشل نتيجة للقص. إذا من المناسب أن كل وصلات الابيام-الأعمدة تتعرض لفشل إنعطافي بتكون المفصلة اللدنة بعيدا عن مناطق تداخل وصلات الأبيام-الاعمدة، تماما في البيم الرابط.

في هذه الدراسة، ثمانية عينات من وصلات الابيام-الاعمدة الركنية الخارجية بمقياس 3/1 من إطار نموذجي مقاوم للعزوم، مكونة من خرسانة عالية المقاومة و بدون تسليح عرضي تم اختبارهم تحت تاثير حمل ترددي بمعدل ثابت باستخدام نظام التحكم في الانحراف (displacement controlled). أربعة من هذه العينات تم تدعيمها بشفة CFRP رابطة في إتجاه واحد بمختلف عدد الطبقات و الاطوال. العينات التي تم إختبارها معمليا تمت نمذجتها بإستخدام أحد البرامج التجارية المتوفرة التي تعمل بطريقة العنصر المتناهي و يدعى ABAQUS. بإستخدام نموذج ضرر الخرسانة اللدن (concrete damage plasticity) و نموذج فشل Tsai-Wu لنمذجة سلوك CFRP و الإيبوكسي معا.

في الاختبار المعملي، العينات المرجعية فشلت بالإنعطاف نتيجة لتكون المفصلة اللدنة في منطقة تداخل وصلة الابيام-الأعمدة. العينات المدعمة أيضا فشلت بالانعطاف و لكن بتكون المفصلة اللدنة عند منطقة توقف شرائح CFRP. عملية تحويل منطقة المفصلة اللدنة ينتج زيادة عالية في القدرة التحميلية، زيادة الممطيلية، و تبديد الطاقة في هذه العينات. عملية النمذجة اللاخطية بإستخدام طريقة العنصر المتناهي أظهرت نتائج مشابهة لتلك التي حصل عليها معمليا. النتائج المعملية و العددية تمت التحقق منها بالطرق التحليلية باستخدام معادلات مواصفات معهد الخرسانة الأمريكي (ACI 440)، بقارنة الحمل الأقصى، و الانفعالات في حديد التسليح و شرائح CFRP.

عملية التدعيم المقدمة في هذه الدراسة مناسبة للمباني الحالية، و هي لا تزال ضرورية للتعرف على كيفية تصميم وصلات الأبيام-الأعمدة للإطارات المقاومة للعزوم لجعل المفصلة اللدنة تتكون داخل الأبيام في المباني المراد إنشاءها

CHAPTER 1

INTRODUCTION

1.1 General

Buildings are designed to withstand the moment induced as a result of loading such as wind, earthquake or even due to building geometry. Moment-resisting frames are made of beams, columns, and beam-column joints. A beam-column joint as defined by Moehle **[1],** is that part of the RC-column which lies within the depth of the deepest beam that frames into the column. The beam-column joint (BCJ) in reinforced concrete construction is considered the most important region in the reinforced concrete frame, as it is the critical element prone to large forces when there is a severe ground shaking. The behavior of the BCJ has a great influence on the response of the structure, namely with reference to its ductility and energy dissipating capability. The beam-column connections enable forces and moments to be transferred among the beams and columns. In modern design codes for earthquake resisting frame, it is a primary objective that the beam-column joints remain essentially elastic while plastic hinges form in adjacent framing members. This framing action can result in relatively large shear forces being transferred across the joint. The location of the plastic hinge formation in BCJ during seismic will determine the mode of failure of the building frame. While shear failure is a global failure which may lead to the outright collapse of the building, flexural failure of the interconnecting beam is desirable

because it is a local failure. Formation of the plastic hinge at the interface of the BCJ is also not desirable because of its penetration inside the core of the BCJ which may lead to shear failure. From the foregoing, it is desirable to have plastic hinge formed at a distance inside the beam. In a new construction, it is quite easy to achieve that, but in traditional building, this could only be achieved by retrofitting of the frames.

1.2 Motivation

Design codes have evolved over the years on how to improve the capacity of nonseismically designed building design for ductile behavior, such codes include ACI 352 [**2]** committee recommendation. Design codes started enforcing stricter seismic provisions for the detailing of reinforcing bars in the joint regions as they remain extremely vulnerable during earthquakes and might result in structural collapses Saatcioglu et al. **[3]**.

Despite these enforcements, many low rise buildings in the Kingdom of Saudi Arabia as well as other regions with low seismic activities are yet to adhere to the recommendation of the ACI 352 committee. Some believe that the use of high strength concrete for construction is adequate for seismic resistance building, while some are completely ignorance of the need for seismically design and detailed RC moment resisting frame.

The earthquake that occurred in Saudi Arabia within the last few years has raised a concern for the government and authority on the need to check traditional and new buildings in the Kingdom for performance against future occurrence of earthquake. In most of the buildings affected by earthquake, the interface of the BCJ has always been the location where plastic

hinge is formed, which usually lead to a global failure of the buildings, as shown in Figure 1-1 and 1-2.

Figure 1-1: Damaged BCJ in Chi-Chi Taiwan, 1999 Earthquake [4]

Figure 1-2: BCJ failure in Nepal 2015 Earthquake [Google website]

The location of the plastic hinge determines the mode of failure of BCJ in moment resisting frames. Therefore, it is necessary to make sure that the plastic hinge forms inside the beam such as to keep the BCJ safe during earthquake.

1.3 Need for Research

In the last thirty years, numerous research has been conducted on behavior of BCJs under seismic conditions through experimental and analytical studies. Many international design codes have undergone periodic revisions to incorporate these research findings for modern design. New design and detailing aspects have been incorporated into the code to preclude joint failure. A vast body of research exists for retrofitting of BCJs in old concrete structures using carbon fibers (CFRP) and glass fibers (GFRP). This method of strengthening and retrofitting structures with CFRP is a focus of intensive research.

Several studies have proposed different ways to retrofit deficient BCJs in the past decades for reinforced concrete frames originally designed for gravity loads. Such frames do not have adequate ductility and strength to present a global failure mechanism as a result of cyclic loading conditions. These structures generally do not have transverse reinforcement at the BCJs regions, hence possess inadequate ductility usually refer to weak column/strong-beam. Therefore, retrofitting of non-ductile BCJ built in seismic area have been an important requirement in modern day design philosophy.

1.4 Research Objectives

The main objectives of this research is to study the behavior of externally flange bonded CFRP for retrofitting external BCJ made with high strength concrete under monotonic and cyclic loading, and relocation of plastic hinge formation from the BCJ interface to a distance inside the connecting beam.

The following investigations will be carried out in order to meet the above stipulated objective:

1. Experimental investigation of the behavior of BCJ made with high strength concrete, retrofitted with flange bonded CFRP sheets.
2. To conduct monotonic and cyclic load tests on such BCJ
3. Finite element modeling of the BCJ in ABAQUS for verification of the experimental results.
4. Analytical validation of experimental and finite element models using mechanistic equations.

CHAPTER 2

LITERATURE REVIEW

2.1 Introduction

ACI-ASCE Joint Committee 352 [**2]** has given design guidelines on the need to study BCJ built before the new seismic code, and methods of repairing and strengthening such deficient joints in other to make them withstand the lateral loading due to seismic actions. Such methods of repair and retrofitting include: use of epoxy; complete removal of deficient section and replacing with new material of required property and strength; concrete jacketing using UHPC, and or the use of FRP. This section provides a comprehensive review of principles, mode of failure and methods of repair of deficient BCJ available in literatures. Experimental, numerical and mechanistic study reviews are presented here.

2.2 Background

A survey of building collapse around the world due to earthquake has shown that the BCJ of external frame is always the first to fail whenever earthquake occurs. Such failure usually leads to partial or complete failure of the building, especially if the frame does not possess adequate ductility to withstand the inelastic deformation that do occur during earthquake. Some damaged BCJ are shown in Figure 2-1.

Figure 2-1: Complete collapse of building in Northridge, California due to deficient BCJ. [5]

In 1963, the Structural engineer association of California (SEAOC) introduced ductile requirements for multistory buildings that are above 48 meters in order to mitigate against collapse of building due to earthquake, this requirement was later extended to all buildings in the seismic zone. Many regions were also classified into seismic zones and areas for proper seismic load estimation. The requirements of SEAOC was later developed and compiled as the Uniform Building Code (UBC) of 1976.

Many countries around the world have followed the USA in developing design guidelines for designing buildings to meet the required ductility expected for moment resistant frames. Despite the design guidelines, traditional building built before the implementation of the

codes are deficient in seismic. It is not economical viable to demolish such building, the need for repair and retrofit is therefore necessary.

The region where columns intersect beams are termed BCJ. The continuity of reinforcement from the column and the beam usually lead to congestion of reinforcement at the BCJ, especially for multistory buildings. While self-consolidating concrete (SCC) has been developed to solve reinforcement congestion problem, it is a well-known fact that concrete is weak in tension and cannot withstand the tensile stresses generated at the joint of BCJ. that are common to beams at their intersections are called BCJs with some joints having limited shear force carrying capacity, especially if the compressive strength of concrete used is not very high when forces larger than these are applied during earthquakes, joints are severely damaged. Repairing damaged joint is difficult, and so the damage must be avoided by designing joint to resist earthquake effects.

Composite polymer has gained popularity in retrofitting and repair of structures in the recent time. Both FRP and TRM materials are termed continuous fibre composites or advanced composites or simply composites. A typical unidirectional stress-strain diagram for steel and FRP under short term monotonic load is shown in Figure 2-2, to compare the characteristics of FRP with steel.

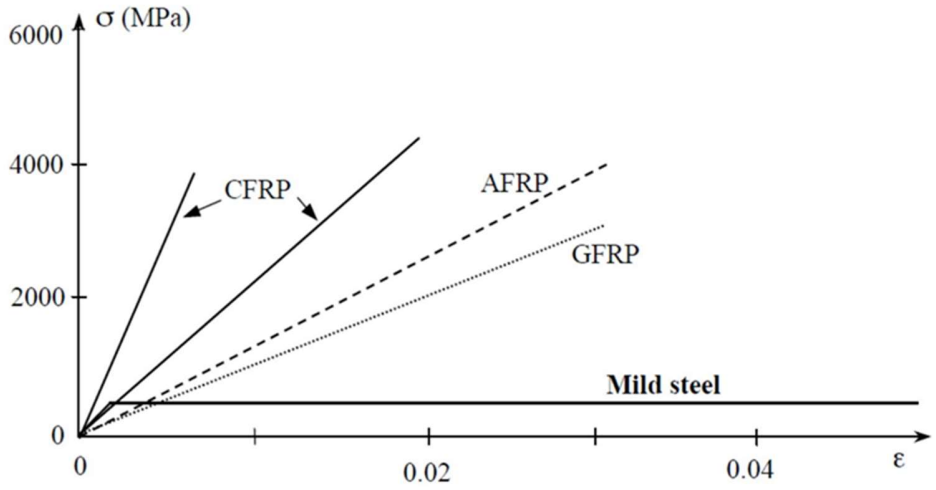

Figure 2-2: Typical stress-strain curve of composite materials used for strengthening.

The very high tensile strength (both static and long term) of composite made it suitable for use in repair and strengthening. Apart from the high tensile strength, the stiffness can be tailored to design requirements; large deformation capacity; immunity to corrosion; availability in different sizes. Despite these advantages, composites have their shortcomings unlike steel which behaves in an elastoplastic manner, composites are linear elastic to failure (although the latter occurs at large strains) without any yielding nor plastic deformation leading to reduced (but typically sufficient) deformability at ultimate. Some fibre materials such as carbon and aramid have incompatible coefficient of expansion with concrete. As a result, exposure of FRP to high temperature in case of fire may lead to premature degradation or collapse (some of the epoxy resins start softening at 45-70 ^{0} C), also the cost of composite per unit weight is several times higher than that of steel (but when cost is based on strength basis, it is cheaper than steel).

2.3 Behavior of BCJ

Research on BCJ can be dated back to 1970, after incessant collapse of reinforced concrete building structures due to earthquake. Among the early research group in this area of study is the Pacific Earthquake Engineering Research (PEER) group at the university of California Berkeley. the major factors that govern the behavior of BCJ include material properties from which the BCJ is made of, type and amount of reinforcement, anchorage and geometry of reinforcement, bond between the concrete and steel reinforcement, presence of beams for confining the joints, and the loading conditions. Combination of those factors give rise to different failure modes which are possible in BCJ. Hassan **[6]** grouped such failure modes into the following categories:

i. Joint failure: This is usually a pure shear failure of the BCJ, such failure is a brittle mode of failure, and represents most building built before the advent of new seismic design code.

ii. Beam Joint failure: the failure mode is initiated by the yielding of the beam top or bottom reinforcement. The yielding penetrates into the core of the BCJ, damage the bond between the reinforcement and concrete, and subsequently lead to joint failure mode, since shear strength is dependent on flexural capacity of the beam.

iii. Column Joint failure: this is initiated by yielding of column reinforcement and penetrates the joint to cause excessive damage in the column. The column joint failure can lead to global failure of a structure if instability is not checked for during the design stage of the building.

iv. Beam-Column Joint failure: this is a combination of beam joint failure and column joint failure. In this failure mode, both the beam and column reinforcement yield simultaneously followed by joint shear failure.

v. Anchorage failure: this mode of failure is caused by bond slip failure of the beam reinforcement or insufficient embedment length of the beam reinforcement inside of the BCJ as the joint will not be able to develop its full capacity under loading.

vi. Axial load failure: this usually occur in BCJ under high axial load in which the column crushes before the joint failure. Numerous studies are still ongoing to determine the effect of axial load on joint shear capacity.

2.4 Experimental studies on BCJ

Hakuto et al. **[7]** conducted a test on corner and interior BCJs which were designed to simulate traditional building without reinforcement at the joint and retrofitting of interior BCJs to improve the ductility as shown in Figure 2-3, the corner BCJ investigated were of different reinforcement detailing configuration for top and bottom beam reinforcement. Traditionally, beam reinforcements end is either bent in or bent out to form hooks in joint. It was concluded that the reinforcement configurations used improved the ductility and shear behavior of the BCJs with reinforcement detail as shown (Figures 2-4 and 2-5)

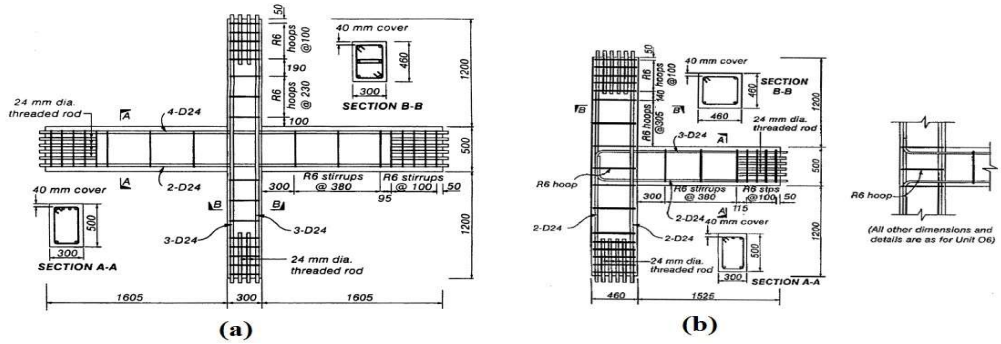

Figure 2-3: Interior and Corner BCJ Reinforcement Configuration [8]

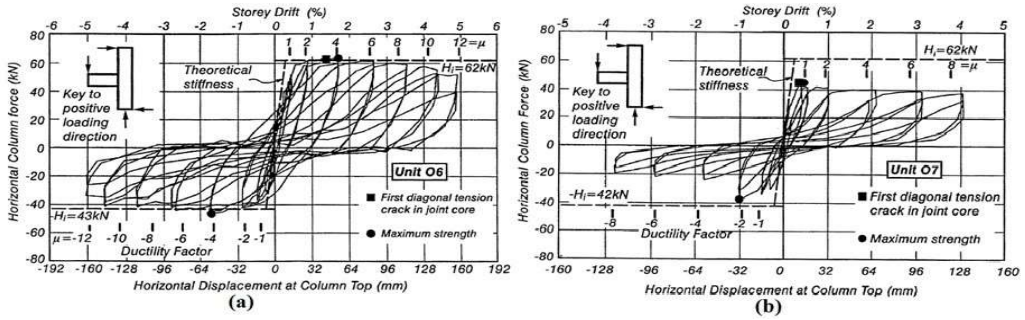

Figure 2-4: Lateral column force-displacement curve for different reinforcement configuration (a) bent down and (b) bent Up Specimen [8]

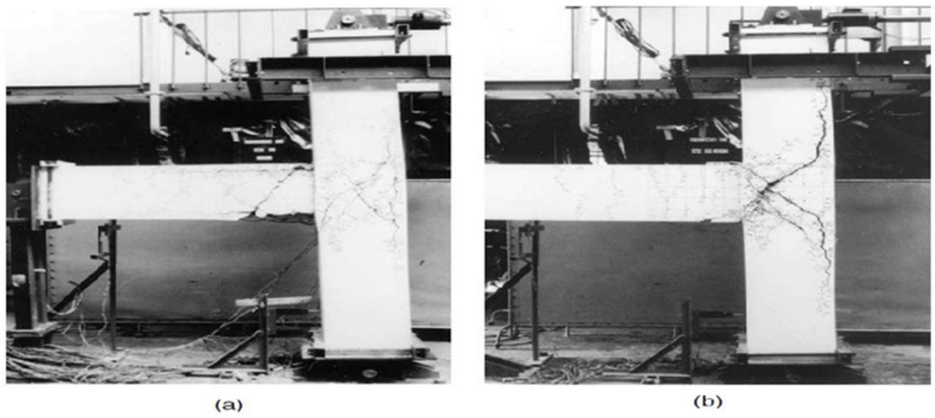

Figure 2-5: Failure mode for (i) Bent Down (ii) Bent up samples [8]

Le-Trung et- al. **[8]** conducted an experimental study on eight external RC BCJ strengthened with different configuration of FRP by applying such FRP on the web, and core region of seismically deficient BCJ. It was concluded that the FRP improved the capacity and ductility of the specimen tested.

Eslami et-al **[9]** carried out a study on the appropriate anchorage system for flange bonded CFRP in retrofitted reinforced concrete BCJs. From the study, the problem and difficulties that do arise from web-bonded CFRP sheets was solved by using flange bonding as shown (Figure. 2-6). In addition, upgrading code-compliant RC joints using a practical FRP scheme was studied. There was remarkable improvement in the load carrying capacity and elastic stiffness of the CFRP-retrofitted specimens which confirm the efficiency of the suggested system. Furthermore, the plastic hinge was relocated away from the beam-column interface, however, the major issue of concern was how to provide adequate development length from the critical section to transfer the FRP tensile forces from beams to columns and vice versa.

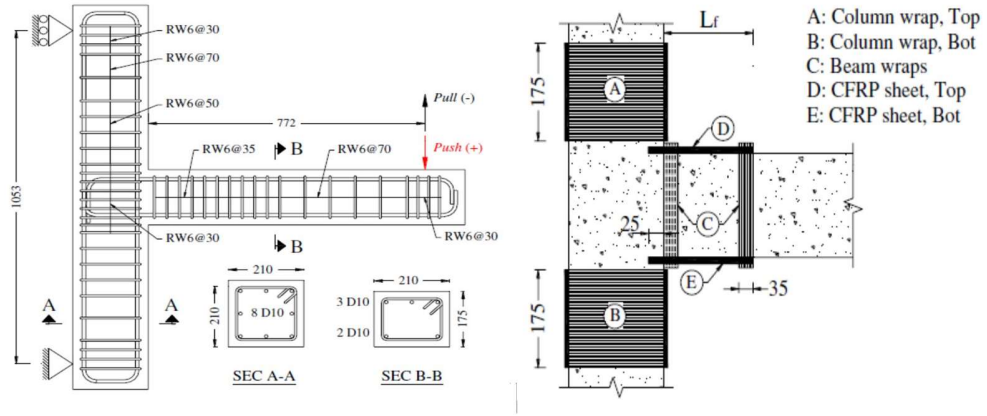

Figure 2-6: Typical configurations for beam-column joints strengthening (a) geometry and reinforcement details of test specimens (b) flange-bonded retrofitting scheme [9].

Danish **[10]** conducted a research on the retrofitting of exterior BCJs using CFRP. He stated that the failure mode of exterior BCJs tested in cyclic loading depends on the beam, column and joint geometry as well as amount of reinforcement and reinforcement detailing of the joint. For the strengthened BCJs with CFRP, its load carrying capacity increased by 13%. The shear stress of the retrofitted BCJ decreased, the failure mode of the CFRP

retrofitted samples changed and concrete cracking failure occurred at the BCJ interface without significant cracks in the joint.

Franco et al **[11]** carried out a study on the inelastic seismic behavior of reinforced concrete buildings built in the 70's undeformed rebar and low compressive strength for the concrete column by testing some interior and corner BCJs under increasing cyclic horizontal drift till failure occurs. It was reported that failure occurred by slipping of the longitudinal reinforcement and by shear failure for the exterior BCJ as shown (Figure 2-7).

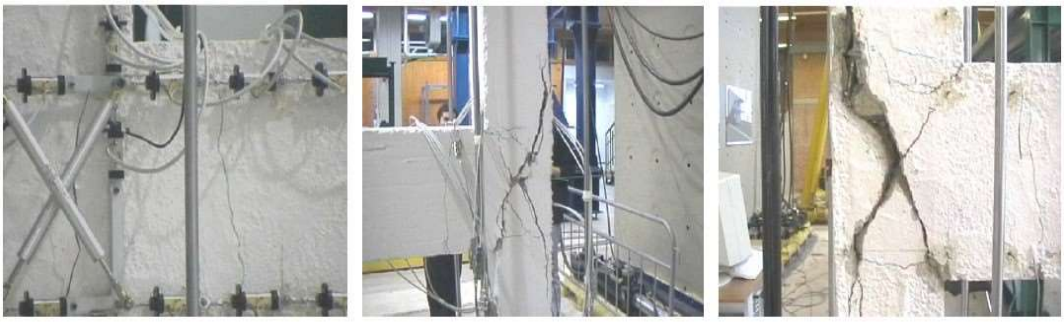

Figure 2-7: Corner-Joint Specimen: Beam and Joint Panel Cracks Pattern at Failure [11]

Chris et al **[12]** tested some corner BCJ with control specimens and retrofitted specimens as shown (Figure2-8). The samples were tested under monotonic and cyclic loading. The performance of such BCJ were studied for load carrying capacity, ductility ratio, etc. The FRP retrofitted BCJ showed a significant improvement in measured capacity as shown (Figure 2-9). It was concluded that the shear strength of the BCJ retrofitted with FRP joint increased by 45% as compared to the control specimens.

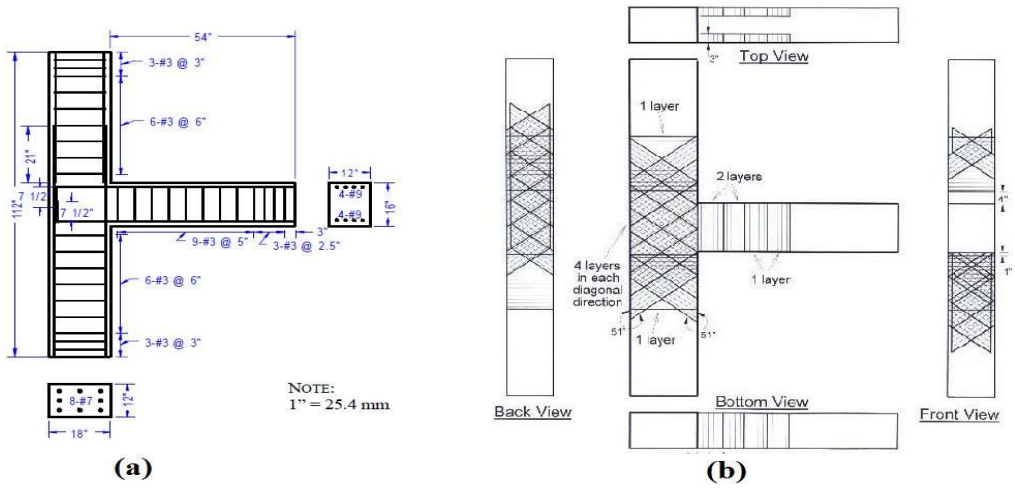

Figure 2-8 : Specimen configuration (b) CFRP Retrofitting Layout [12]

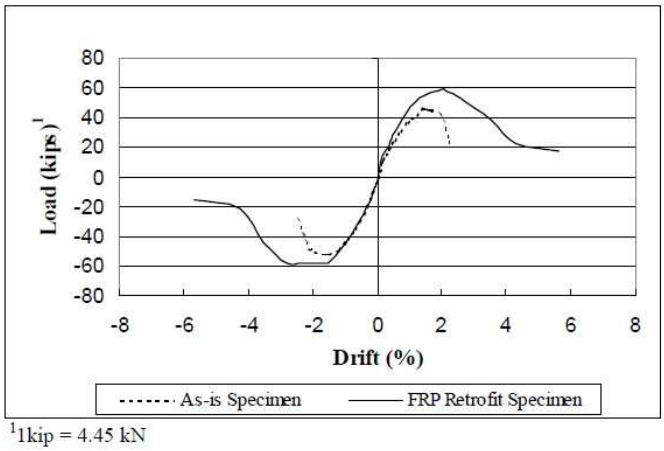

Figure 2-9: Load displacement Curve for control and FRP Retrofitted Specimen [12]

Kien et-al. **[13]** studied eight 1/3 scale corner BCJ with different CFRP retrofitting scheme shown in Figure 2-10, to determine the most efficient configuration of CFRP strengthening technique for improving the lateral strength and ductility of the BCJs.

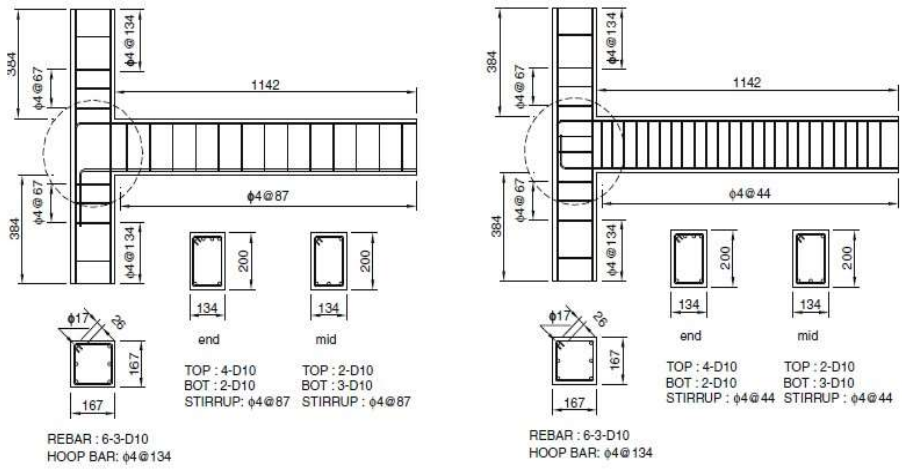

Figure 2-10: unreinforced joint and (b) reinforced joint Details for the specimens [13]

Ravi et al. **[14]** carried out an experimental study on effect of development length in retrofitted BCJs. Nine specimens were cast, in which six were designed and detailed according to IS 456:2000 Code. The other three were designed and details to IS 13920:1993 as shown in Figure 2-11. Retrofitted specimens were made according to code IS 456:2000. Three of the retrofitted specimens were wrapped with GFRP and other three with CFRP. The control and retrofitted specimens were tested for static loading. It was reported that the load carrying capacity increased by 14.5%, and 10% in energy absorption as given in Figure 2-12.

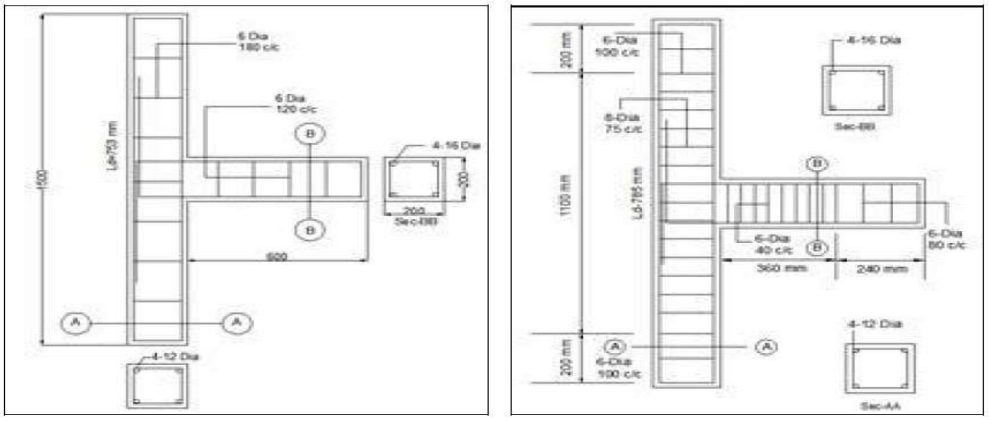

Figure 2-11: Reinforcement configurations to (a) IS 13920 (b) IS 456 Samples Configuration [14]

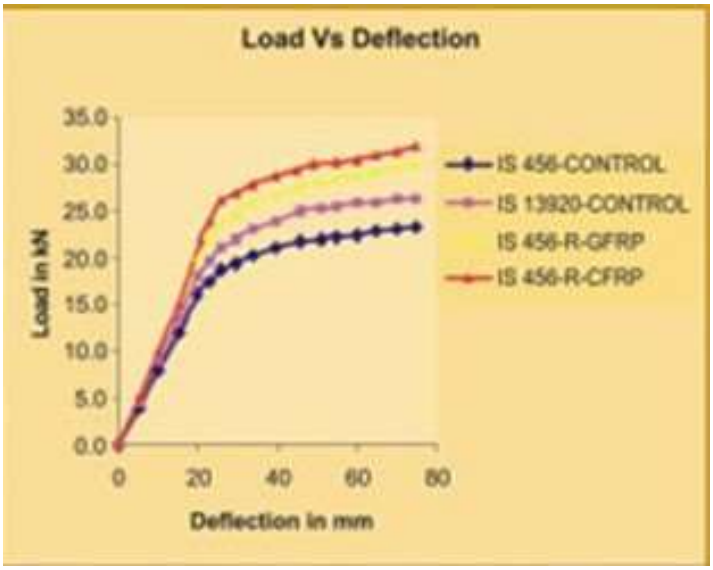

Figure 2-12: load Displacement Curve for tested Specimens [14]

Ghobarah et al. **[15]** carried out an experiment on exterior unreinforced BCJs under cyclic loading, for control and retrofitted samples using GFRP as shown in Figures 2-13 and 2-14. Their results showed that the retrofitted samples did not fail by brittle joint failure noticed in the control samples as shown (Figure 2-15).

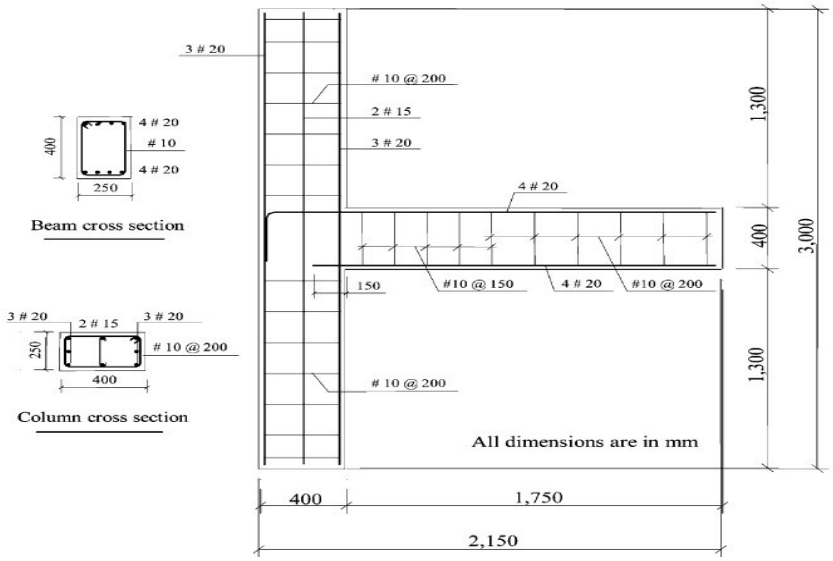

Figure 2-13: BCJ Configuration [15]

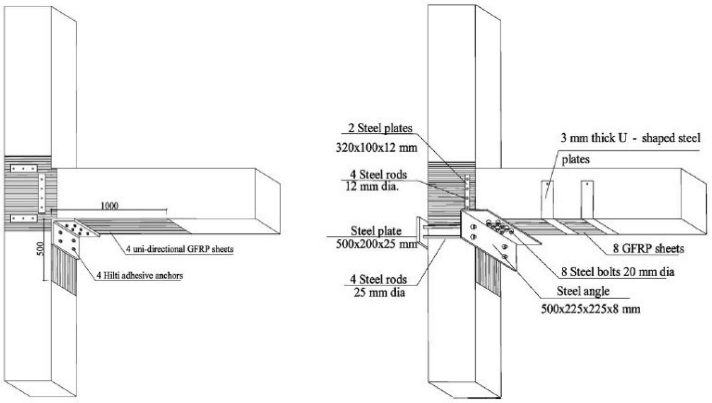

Figure 2-14: CFRP configuration for retrofitting BCJ [15]

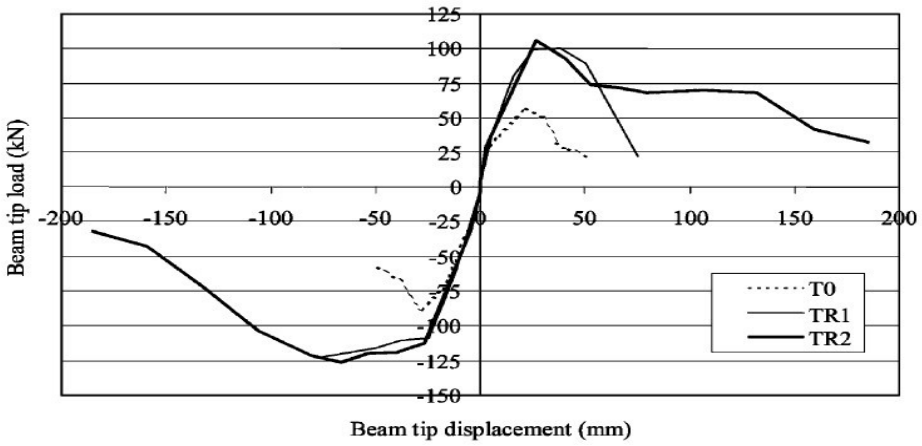

Figure 2-15: Hysteretic Loop Envelopes of the Tested Specimens [15].

Sasmal **[16]** studied different techniques of retrofitting BCJ subjected to cyclic loading, the BCJ samples were designed for seismic loading according to Indian standard without ductility consideration and repaired with epoxy mortar and grout using low viscous polymer and retrofitted with FRP wrapping as shown (Figure 2-16). It was reported that there was an increase in stiffness of the retrofitted specimens and 25% increase in cumulative energy dissipation as shown (Figure 2-17).

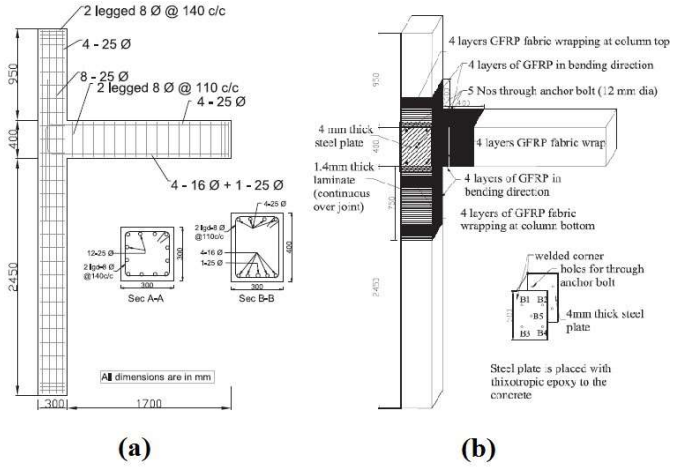

Figure 2-16: Configuration of (a) non-ductile' Specimen and (b) Retrofitting scheme for damaged 'Non-Ductile' specimen [16]

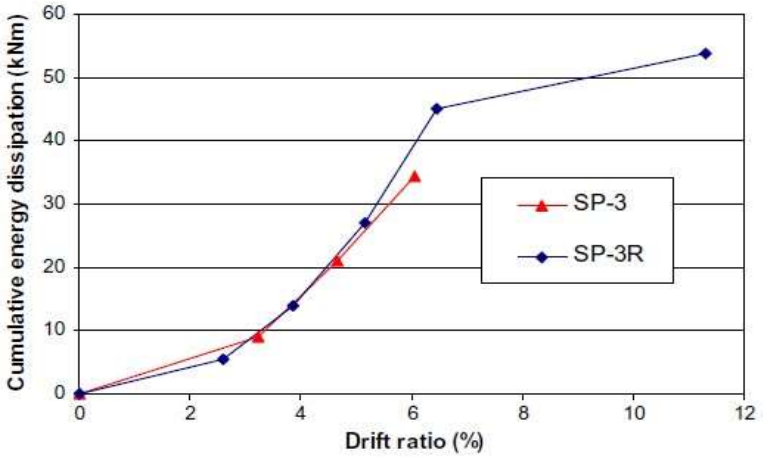

Figure 2-17: Comparison of Cumulative Energy Dissipation [16]

Al-Sayed et al. **[17]** reported a new approach for retrofitting poorly detailed corner BCJ by FRP composites (Figures 2-18 and 2-19). A full scale corner BCJ sub-assemblage was used without transverse reinforcement in the joint and tested under reversed cyclic lateral load. It was reported that there was increase in load capacity, ductility, etc. the BCJ (Figure 2-20) displayed a slower loss of stiffness after FRP retrofitting.

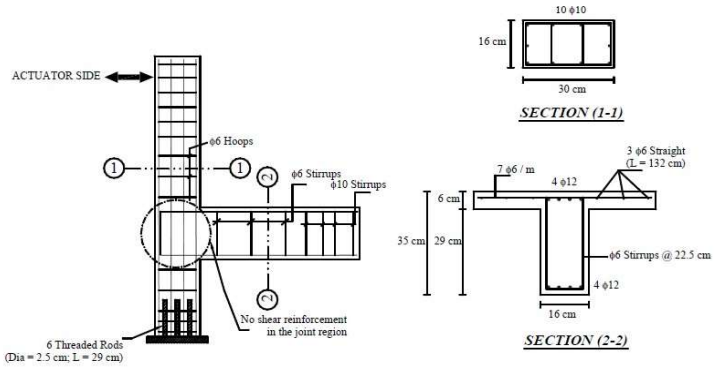

Figure 2-18: BCJ tested samples with rebar detailing [17]

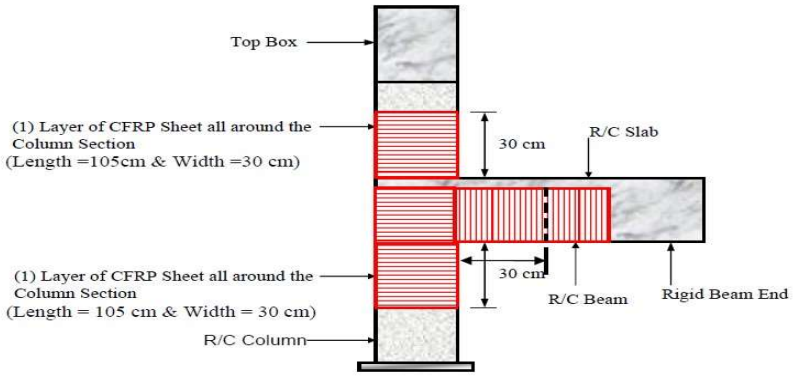

Figure 2-19: Approved configuration of FRP for corner BCJ [17

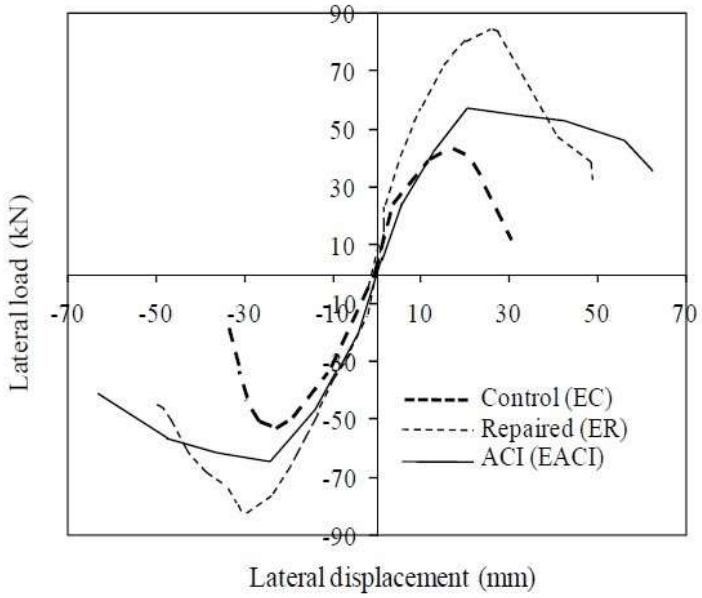

Figure 2-20: Envelopes of Hysteretic Plots for As-Built Control, Repaired and ACI Based Designed Specimens [17]

Failure mode of normal and CFRP retrofitted BCJs designed to fail in flexure in beam and diagonal shear failure in joints using conventional concrete of 30MPa was conducted by Halahla **[18]**. BCJ were made with reinforcement sizes of 18mm and 12mm. the failure mode of CFRP retrofitted BCJ-18mm changed to a ductile mode from the brittle joint shear failure while for BCJ-12mm, the failure mode remains as flexural failure in non-retrofitted

and retrofitted specimens but the first flexural crack occurred outside the BCJ interface. BCJ-18mm ultimate load capacity increased by 13%, while BCJ-12mm increased by 10%.

Hadigheh et al. **[19]** studied the performance of weak -beam, strong-column RC frames strengthened at the joints by FRP experimentally and numerically using ABAQUS. The FRP was applied at the web of the beam, using different layers and tested under monotonic load regime (Figure 2-20). It was observed that the first crack occurred after the termination of the CFRP length, and there was an increase in the load carrying capacity, as well as first yielding of steel in the retrofitted specimen.

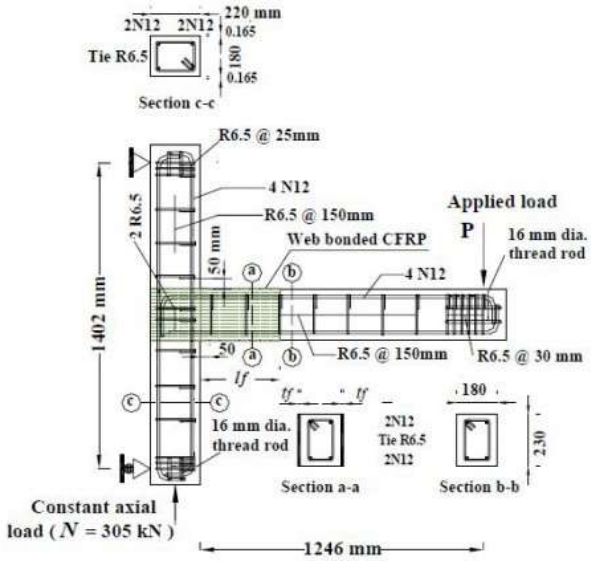

Figure 2-21: Retrofitted BCJ configuration [19]

Hadi et al. [20] conducted an experimental study on repair and retrofitting nonseismically detailed exterior BCJ using concrete cover with CFRP jackets. Two samples of BCJ without transverse reinforcement at the joint was retrofitted and repaired, using CFRP and concrete cover to modify the square shape of the BCJ specimen to circular cross-sections (Figure 2-22). Increase in load carrying capacity, stiffness and energy dissipation was observed after the test, although the retrofitted specimen had a better performance than the

repaired specimen which is due to the fact of the yielding of the beam longitudinal reinforcement.

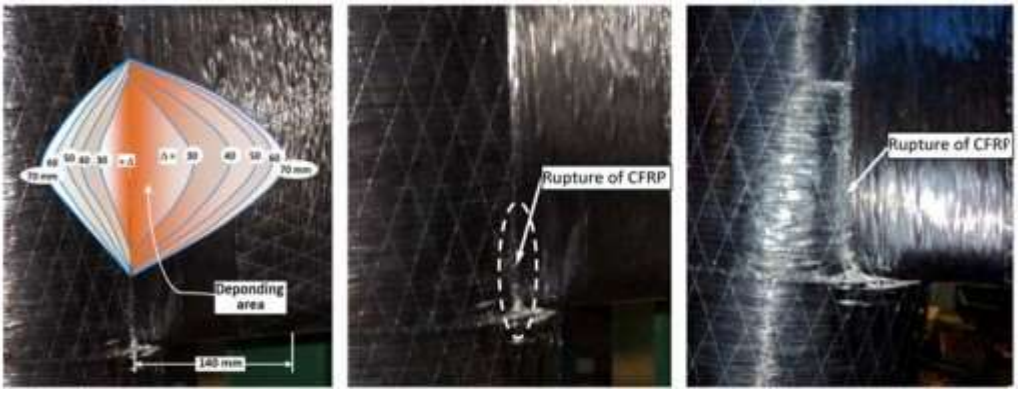

Figure 2-22 : Retrofitting configuration of BCJ [20].

From the above discussions, there exist a large documentation of BCJ failure as a result of various factors. Table 2-1 below summarizes all these factors for unreinforced joint of BCJ.

Table 2-1: Summary of Experimental Results for unreinforced BCJ

References	Specimens tested	Joint Type	Joint Aspect Ratio	f_c'	f_y	Beam ρ_b	Column ρ_c	Mode of failure
Hadi **[20]**	TS & TR	Ext.	1.5	50.0	500	0.75	3.0	J
Wong **[21]**	JANN03, JANN15, JBNN03	Ext.	1.3	46.0	520	0.46	2.25	BJ
Gogkoz **[22]**	US-3 & US3 ES	Ext.	1.67	23.5	441	0.59	2.1	J
Barnes **[23]**	SP 1 & 2	Ext.	1.5	46.1	469	1.94	3.2	BJ
Clyde et al. **[24]**	SP 2, 4,5 & 6	Ext.	0.89	41.0	469	2.45	2.23	J
Hakuto [8]	06 & 07	Ext.	1.10	31.0	308	0.66	0.86	J

Ghobarah et al. **[15]**	T1 and T2	Ext.	1.0	30.9	425	1.2	1.8	BJ
Pantelides et al. **[25]**	01,02,03,04 ,05, and 06	Ext.	1.0	34.0	469	1.9	2..45	J
Karayannis et al. **[26]**	A0, B0 & C0	Ext.	1.0	31.2	580	0.85	1.89	BJ
Engindenz **[5]**	SP 1-NS, SP 1-EW, SP 2-NS, SP2-EW	Ext.	1.43	34.6	315	0.78	1.68	J
Antonopoulos et al. **[27]**	C1 & C2	Ext.	1.0	22.0	460	0.77	1.54	J

Note: Failure mode J: Joint shear failure mode without yielding of beam reinforcement, BJ: Joint shear failure with yielding of beam reinforcement, BF: Beam flexural failure.

2.5 Factors governing the behavior of BCJ.

In this section, the major factors governing the behavior of BCJ are discussed using Table 2-1., as a reference. These three factors are: (i) Joint Aspect ratio, (ii) Beam reinforcement, and (iii) Axial load on Column

Many researchers have studied the effect of joint aspect ratio experimentally. For an exterior BCJ with transverse reinforcement at the joint, Kim et al. **[28]** an aspect ratio from 1.0 to 1.6 had little influence on the joint shear stresses and strains for BCJ failing by joint and yielding of the beam reinforcement. Also, it was reported that an increase in aspect ratio reduce the shear strength of the joint for BCJ failing by joint shear failure without yielding of reinforcement. Wong **[21]** reported that for BCJ without joint shear reinforcement, and having aspect ratio ranging from 1.0-2.0, the joint shear strength is

inversely proportional to the aspect ratio in conformity with previous studies of Bakir et al. **[29]** and Vollum et al. **[30].**

Anderson et al. **[31]** observed that the failure mode and joint strength of BCJ depend on the beam reinforcement ratio and the joint shear stress demand, but not on the shear strength of the joint. The observations are similar to that observed for exterior BCJ without transverse reinforcement at the joint studied by Wong **[21]**. Wong **[21]** had reported that BCJ with high amount of beam reinforcement would failed by joint failure, without yielding of the beam reinforcement. In BCJ without transverse reinforcement, the increase in joint strength as a result of increase in beam reinforcement is due to increased compression force in the diagonal strut with little loss of bond stress, as there is no mechanism to transmit joint shear horizontally.

The exact way axial load on column affects the behavior of BCJ is still not well known. While some authors reported that there is negligible effect of BCJ on joint shear strength, others believe that there is an increase in joint shear strength due to high axial load, Park et al. **[32]**. For a BCJ designed as weak column–strong beam, increase in axial load till a balanced point will result into higher joint shear strength, because the column moment capacity is dependent on the axial load, but for a BCJ with, strong column–weak beam, it has been reported that increase in axial load has a combined effect on shear strength. Using strut-and-tie model, increase in column axial load will compression block depth if the joint which will result in increase in joint shear strength. This increase in compression block depth also improves the bond resistance between the concrete and beam reinforcement. In contrast, high column axial load can lead to crushing of the column and the joint which can

be make the joint susceptible to failure under loading. Hence, there is a need to strike an equilibrium on axial load effect, Park et al. **[32]**

2.6 Shear strength models

Even though the focus of this research is on retrofitting of BCJ using externally flange bonded CFRP for plastic hinge relocation, some existing mechanistic models on shear strength of BCJ are reviewed in brief. Only the most critical and widely used models are discussed.

i. Bakir and Boduroglu Model

Bakir and Boduroglu proposed an empirical model for predicting the shear strength of BCJ based on joint aspect ratio, beam reinforcement ratio, amount/presence of transverse reinforcement at the joint, and anchorage details. The empirical relation was developed from parametric study conducted on BCJ.

$$V_c = 0.71\beta\gamma \left(\frac{100A_{sb}}{b_c d}\right)^{0.4289} \left(\frac{b_c+b_b}{2}\right) \left(\frac{h_b}{h_c}\right)^{-0.61} \sqrt[h_c]{f_c} + \alpha A_{sje} f_y \qquad (2.1)$$

β is 0.85 beam reinforcement having a U shaped anchorage, and 1.0 for a 90-degree bend.

γ is 1.37 for joints having inclined bars, and 1.0 for others.

α is 0.664 for BCJ with low amount of transverse reinforcement, 0.6 for medium and 0.3 for high amount of reinforcement.

ii. Vollum and Neumann Model

The authors empirically estimated the joint shear strength as

$$v_j = v_c + \left(A_{sje} f_y - \alpha b_{eff} h_c \sqrt{f_c}\right), \quad (2.2)$$

$$v_c = 0.642\beta \left(1 + 0.555\left(2 - \frac{h_b}{h_c}\right)\right) b_{eff} h_c \sqrt{f_c} \quad (2.3)$$

In no case should

$$v_j < 0.97\left(1 + 0.555\left(2 - \frac{h_b}{h_c}\right)\right) b_{eff} h_c \sqrt{f_c} < 1.33 b_{eff} h_c \sqrt{f_c} \quad (2.4)$$

v_j is the total shear strength of the joint in the presence of joint transverse reinforcement, α is a function of joint aspect ratio, column reinforcement ratio, and grade of concrete. β is 1 for 90-degrees, and 0.9 for a U shaped reinforcement.

iii. Ilki et al. Model

Ilki et al. **[33]** proposed a model for computing shear strength of BCJ, the model does not consider the contribution of joint aspect ratio and beam reinforcement, rather, it considers the effect of axial load on the column. According to this model, the axial load increases the BCJ shear strength. The model gives

$$\tau_{vc} = 0.5\sqrt{f_c}\sqrt{\left(1 - \frac{N}{0.5\sqrt{f_c}\, A_g}\right)}; \quad (2.5)$$

$$\text{and } V_c = \tau_{vc} bd$$

iv. Sarsam and Philips Model [34].

This model was empirically fixed from experimental test conducted on BCJ under monotonic loading. The model considered different parameters contributing to the shear strength. The shear strength is given by,

$$V_j = 5.08(f_c{}'\rho)\left(\frac{d_c}{d_b}\right)^{1.33}\left(1 + 0.29\frac{N}{A_g}\right)^{0.5} b_c d_c \quad (2.6)$$

v. ACI-Design guidelines [2].

The nominal joint shear strength according to the ACI-352 committee recommendation is given by;

$v_n = 0.083\gamma\sqrt{f'_c}\, b_j h_c$, where bj is the effective joint width, h_c is the column depth in the direction of the load, b_j is the least of $\begin{Bmatrix} \frac{b_c + b_b}{2} \\ b_b + \sum \frac{mh}{2} \\ b_{col} \end{Bmatrix}$, m is the co-efficient for effect of eccentricity as given in the ACI 352 code, and γ is a factor for the effect of confinement of the joint. From the above expression for the joint shear strength, the effect of the beam reinforcement and axial load on the column are neglected.

2.7 Review of numerical studies on BCJ.

Experimental studies are believed to be the best form of testing reinforced concrete structures under loading because of the nonlinearity behavior of concrete, which is difficult to simulate numerically, but the challenges involve in experimental studies have raised concern on such beliefs. These challenges include but not limited to cost implication, most experimental studies are destructive in nature, difficulty in fixing and testing of specimens. In other to solve the above problems, finite element based programs have been developed for simulation.

Sagbas **[35]** simulated some models of BCJ using VecTor2 to model. The BCJ simulated were made with smooth steel reinforcement for unconfined BCJ deficient in shear, and its strengthening. Hognestad and modified Park Kent model was used for the concrete, behavior while default linear option was used for tensile behavior of concrete. It was concluded that the observed failure mode for the experimentally studied specimen and that of numerical studies were in good agreement. The load capacity, failure mode, ductility and strains were in agreement.

Mitra et al. **[36]** used DIANA 9.1 to study the behavior of BCJ using Drucker-Prager model for compression response. It was concluded that the material models used are capable of representing behavior of fairly complex problems but with little discrepancies such as inability to capture cracking and crushing of concrete simultaneously as a result of numerical instability algorithms and insufficient martial models in DIANA 9.1 software. Therefore, he recommended the explicit non-linear FE codes like LS-DYNA and ABAQUS for simulation of complex problems considering local inelastic mechanisms.

ABAQUS (2013) **[37]** is a commercially available nonlinear finite element used to simulate and validate different experimental load testing on RC structures and steel structures. It requires materials constitutive and experimental data as input files for it to initiate the analysis.

Hadigheh et al. **[19]** used Abaqus to simulate the experimental studies of Mahini on performance of weak-beam, strong column RC frames strengthened at the joints by FRP, by adjusting the fracture energies of the FRP laminates. The results obtained was in close agreement with that of the experimental studies of Mahini et al. **[38]**. Eslami et al. **[9]** used

ANSYS to simulate their previous experimental studies Eslami et al. **[9]**, using William Wranke concrete model. Similar results were observed from the experimental procedures. Due to these reasons, ABAQUS (2013) was selected in this study for the numerical simulations.

CHAPTER 3

MECHANICS OF BEAM COLUMN JOINT

3.1 Introduction

This chapter focuses on theory and mechanics of beam column joints, and CFRP for retrofitting RC structures. Some mechanistic models for predicting capacity of retrofitted structures are also discussed.

3.2 Configurations of beam column joints

BCJ have different configurations depending on their locations in the external envelope of a moment resisting building frame. In frames where lateral load is the predominant force, it can be assumed that the point of inflexion will be at the mid-height of the vertical supports (both the frame above and below), as shown in Figure 22, and likewise in the beams. One can with such assumption, conclude that only half of the frame needs to be analyzed.

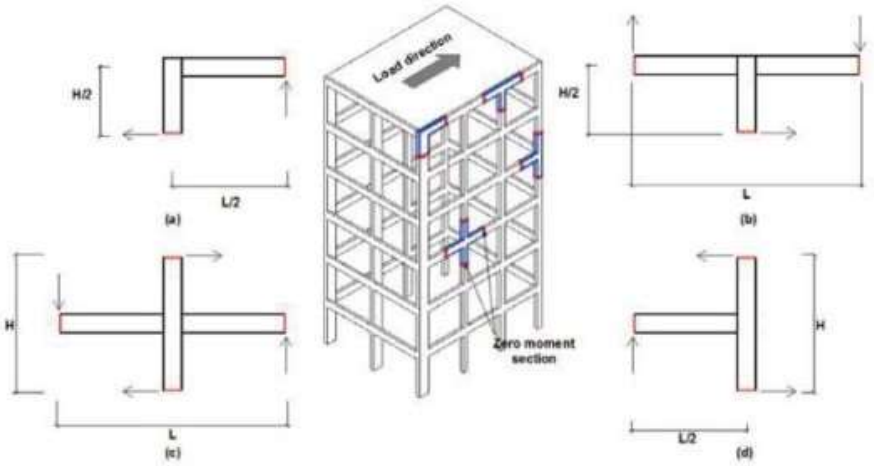

Figure 3-1: Different configuration of BCJ in a MRF building with lateral load parallel to the building axis.

It is the corner external BCJ that suffers most during seismic actions, hence further discussion will concentrate on the external corner BCJ as shown in Figure 3-1.

3.3 Loading action on BCJ

In a corner BCJ under seismic loading, the joint is loaded through the beam reinforcement and the axial load on the column. Figure 3-2 shows a hypothetical BCJ under loading.

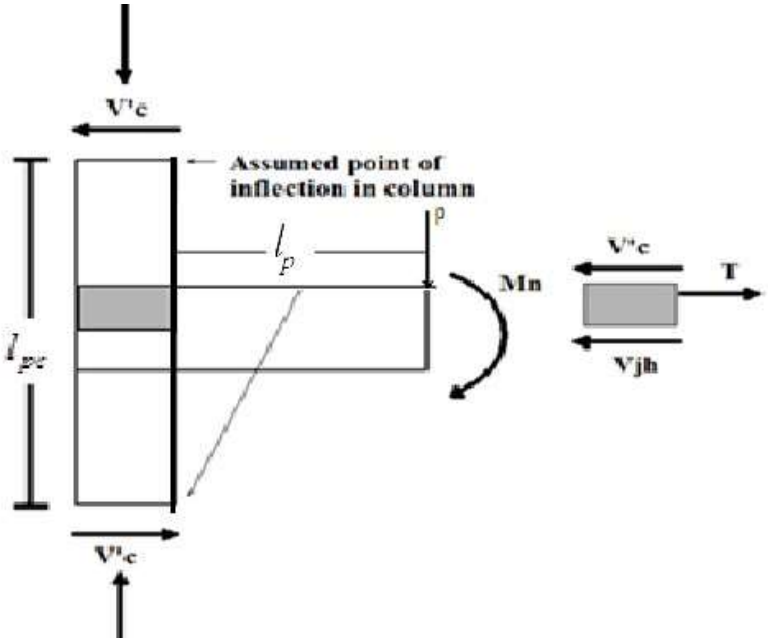

Figure 3-2: Schematic diagram of a loaded BCJ.

The length of the column between the point of inflexion is l_{pc}, while l_p is the span of the beam from the point of loading to the face of the column, P is the concentrated load on the beam and T is the tensile force generated by the top reinforcement of the beam. The moment caused by the load is M_n.

$$M_n = P\ x\ l_p \qquad (3.1)$$

$$V_c' = \frac{M_n}{l_p} \qquad (3.2)$$

$V_{jh} = T - V_c'$ for the equilibrium of the joint in the horizontal direction.

This force can be converted to stress by dividing with the area of core, Aj.

$$v_{jh} = {V_{jh}}/{A_j} \qquad (3.3)$$

and the axial load on the column also generate a stress termed v_{jv}. The axial load on the column creates a normal stress given by σ_N and the beam load creates a shear stress termed τ_v. This state of stress act at any point with the core of the BCJ, as shown in Figure 3-3(a).

If σ_N is taken as σ_x, and τ_v is taken as τ_{xy}, with σ_y taken as zero, the principal stresses can be obtained using Mohr circle as shown in Figure 3-3(b). The principal stresses $\sigma_1 \, and \, \sigma_2$ are given as follows:

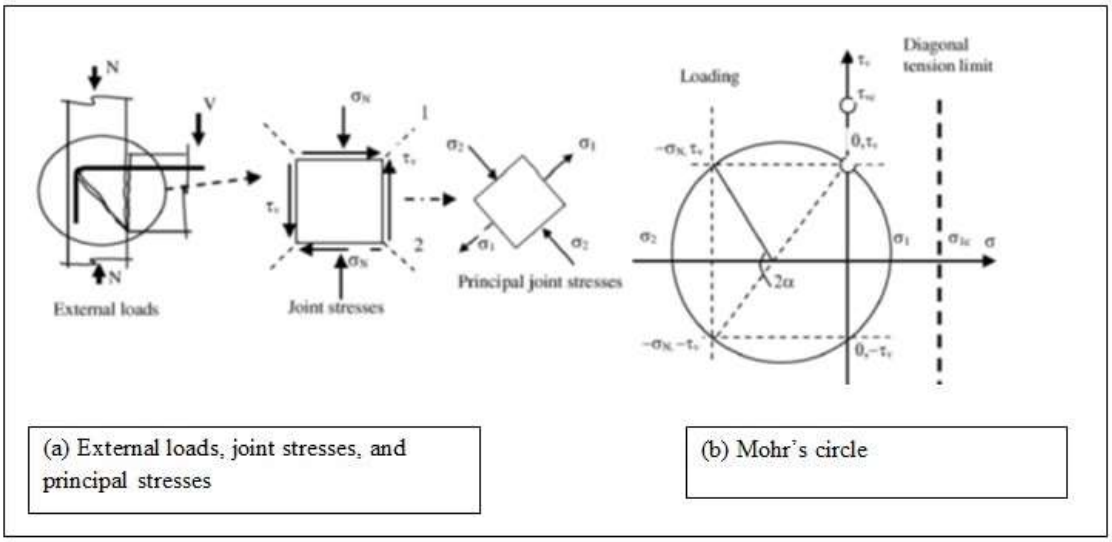

Figure 3-3: Loaded BCJ stresses and Mohr's circle.

$$\sigma_{1,2} = \frac{\sigma_x+\sigma_y}{2} \pm \sqrt{\left(\frac{\sigma_x+\sigma_y}{2}\right)^2 + {\tau_{xy}}^2} \tag{3.4}$$

Since σ_y is zero, and σ_N is N/A_g, equation above becomes;

$$\sigma_{1,2} = \frac{\sigma_N}{2} \pm \sqrt{\left(\frac{\sigma_N}{2}\right)^2 + {\tau_v}^2} \tag{3.5}$$

The limiting stress for crack to occur in the joint is the tensile strength of the concrete, in the absence of shear reinforcement in the joint, assuming that the column crushing of the column does not occur. This tensile strength if taken as $f_t = \sigma_1 = 0.5\sqrt{f_c'}$, then,

$$\tau_{vc} = 0.5\sqrt{f_c'}\sqrt{\left(1 - \frac{N}{0.5\sqrt{f_c'}\,A_g}\right)} \tag{3.6}$$

3.4 CFRP retrofitting

ACI 440.2R-08 **[39]** gives recommendation on CFRP retrofitting of RC structures. Some of these recommendations include maximum useable strain in FRP, mode of failures, and FRP strength reduction factors among others, for an example, a strength reduction factor of 0.85 is recommended for structures retrofitted with externally bonded CFRP that is exposed externally, while 0.95 is recommended for structures internal exposure.

Five modes of failure for flexural strengthening were highlighted depending on the design approach used in retrofitting, but brittle failure usually from rupture of FRP must be avoided. These failure modes are:

i. Concrete crushing before the yielding of steel reinforcement;
ii. Tensile Reinforcement yields accompanied by FRP rupture;
iii. Yielding of tension reinforcement accompanied by concrete crushing;
iv. Delamination of concrete cover; and
v. FRP debonding from the concrete.

ACI 318 **[40]**, gives the maximum allowable compressive strain in concrete as 0.003 to prevent concrete crushing, and once the FRP effective strain reaches its ultimate strain, rupture of the FRP will occur, that is; once ε_f=ε_{fu}. Since FRP are bonded to concrete using epoxy, the tensile strength of the epoxy is the limiting factor for debonding of FRP from the concrete substrate, even if the FRP has not reached its limiting stress. Teng et al. **[41]** equation for the limiting strain in FRP debonding was accepted by ACI 440.2R-08 for FRP design with debonding failure mode.

The debonding strain is given by;

$$\varepsilon_{fd} = 0.41\sqrt{\frac{f_c{}'}{nE_f t_f}} \leq 0.9\varepsilon_{fu} \text{ in SI units.} \qquad (3.7)$$

The mechanistic model used in this study is that recommended in the ACI 440.2R-08.

CHAPTER 4

EXPERIMENTAL PROGRAM

4.1 Introduction

In this chapter, the details of the experimental program conducted at "the Heavy Structures Testing Laboratory" at KFUPM are discussed and reported. The test comprised of eight 1/3 scale exterior BCJ made from high strength concrete, tested under displacement controlled monotonic and reversed cyclic regime. The aims of the test are to study the behavior of BCJ made with high compressive strength concrete, and effectiveness of externally flange bonded CFRP on the BCJ for cyclic loading. All the test specimen had necessary equipment and instrument to measure and record necessary data from the test such as strains, load, displacements, etc.

4.2 Test objectives

The objectives of these experimental program are:

1. understand and study the behavior of BCJ made with high strength concrete,

2. Study the effectiveness of externally flange bonded CFRP on retrofitting such BCJ;

3. Determine most suitable length and number of layers of CFRP required for optimum performance of such retrofitted BCJ.

4. Obtain data required for calibration of FE program using Abaqus, and mechanistic models.

4.3 Design of specimens

In the experimental program, the design of each constituent member were designed according ACI 318-11, by keeping the design parameter constants. the design of each of these constituent elements are done to replicate traditional- to- modern buildings in low seismic region.

4.3.1 Beam reinforcement

From the literature review on factors responsible for mode of failure of BCJ, it was observed that the beam reinforcement plays a major factor on behavior and failure mode of BCJ. Therefore, the beam was designed in such a way that the column reinforcements will not yield prior to failure of the joint which was done by carrying out inelastic section analysis within the range permissible stress for the loading conditions. The beam reinforcement ratio used for all specimen was 0.00804 (for both top and bottom reinforcement). Adequate development length and anchorage were provided for the reinforcement to prevent slipping and premature failure of the beam before reaching its ultimate strength

4.3.2 Column reinforcement design

Just as similar to the beam reinforcement design, the design of the column was based on flexural capacity of the beam, in which it was chosen to be two times that of the beam. This was chosen to prevent yielding of the column reinforcement prior to that of the beam. PCA COL was used to design the column using tension controlled interaction diagram.

4.3.3 Design of the joint

The joint aspect ratio is another major factor that governs the behavior of BCJ. The aspect ratio used in this study was taken to be 1.0. as found in literature, representing a typical concrete frame built in Saudi Arabia. The joint was designed without transverse reinforcement to represent a traditional-modern building designed to traditional design code, but using high strength concrete.

The summary of the design of the specimen is shown in Table 4-1, and the structural detail of the BCJ specimen is shown in Figure 4-1.

Table 4-1: Summary of BCJ design

Specimen	Dimensions (mm)		Reinforcements				
	Beam	Column	Beam			Column	
			Top	Bottom	Stirrups	Long.	Ties
All	250 x 300	250 x 300	3 of 16 Ø	3 of 16 Ø	8 Ø @ 75	6 of 16 Ø	8 Ø @ 75

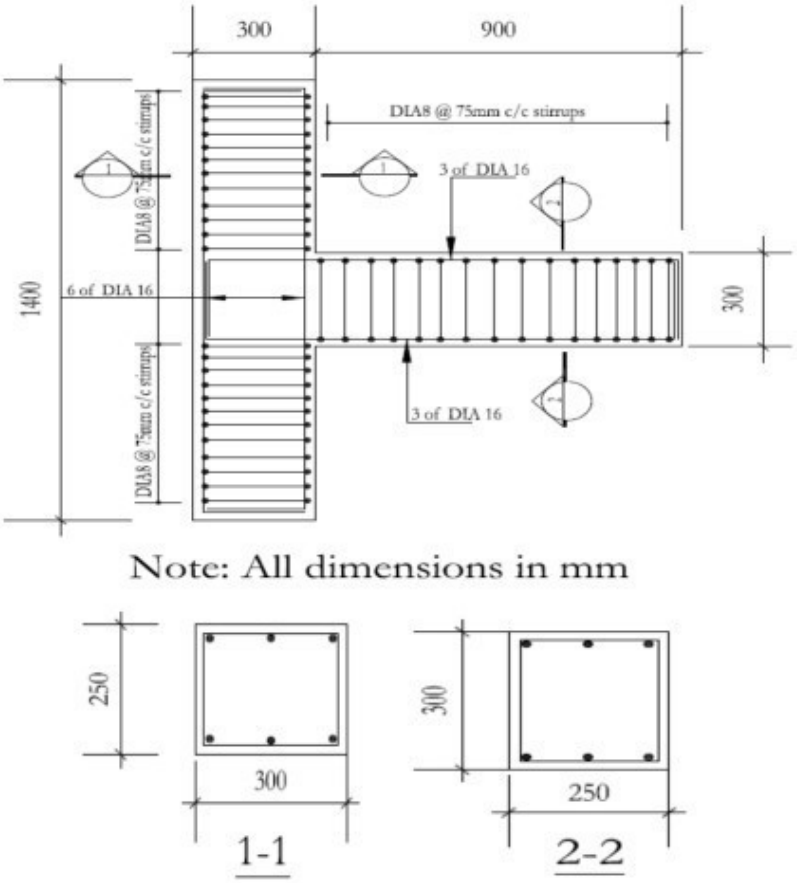

Figure 4-1: Geometric and Reinforcement Details for BCJ

4.4 Construction of BCJ specimens

The BCJ concrete specimens were cast at precast concrete factory, Prainsa in other maintain high quality control in batching, mixing and delivery of fresh concrete. Steel formwork were produced according to dimension and size required for the specimens, with provision for concrete cover and hooks to lift the hardened concrete specimen after construction. Reinforcement cages and steel strain gauges placed on the specimens as shown in Figure 4-2 were produced at the same time for all the 8 specimens for uniformity and same level of workmanship for all the specimens. The concreting was done right in

Prainsa factory for all the specimens as shown in Figure 4-3-4-8 on the same date from the same concrete batch to ensure uniformity in samples and avoid variations in concrete strength due to different batch of Concrete.

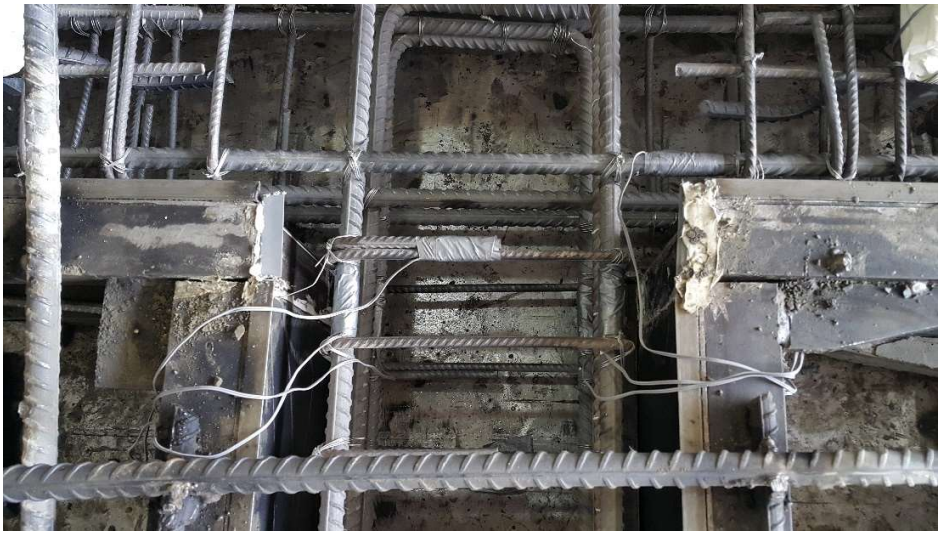

Figure 4-2: Installation of strain gauges and reinforcement cages.

Labelling of the strain gauges and their protection were done during concreting to avoid damaging them. After the specimen were cast, the were properly cured in the factory to ensure that full hydration takes place in order for the concrete specimen to gain full strength, and loss of hydration water to evaporation or humidity. The cured concrete specimens were moved from the factory to heavy structure laboratory of the King Fahd University of Petroleum and Minerals.

Figure 4-3: Fixing of reinforcement cage and lifting hooks

Figure 4-4: Batching and dumping equipment ready for concreting.

Figure 4-5: Dumping of concrete into formwork

Figure 4-6: Vibrating of concrete to prevent honeycomb.

Figure 4-7: Cured specimens ready for transporting.

4.5 Retrofitting schemes

The BCJ specimens were retrofitted after 28 days when the specimens had gained sufficient strength using unidirectional sika Hex 230C and epoxy of Sikadur 330. Different configurations of retrofitting schemes were used with the objective of relocating the formation of plastic hinge from the interface of the BCJ to a distance inside the beam. Of

the eight specimens tested, six had CFRP, while two were used as controls, as shown (Table 4-2).

Table 4-2: Specimens Details

S/No	Details	Number of specimens
1	BCJ without CFRP (Control)	2
2	BCJ with CFRP (Retrofitted)	6

The first configuration has CFRP strips bonded to the web of the BCJ has, others have CFRP sheets bonded to the flange of the beam and the third configuration have CFRP bonded to both the web and the flange of the beam. These configurations are shown in Figure 4-8 and 4-9.

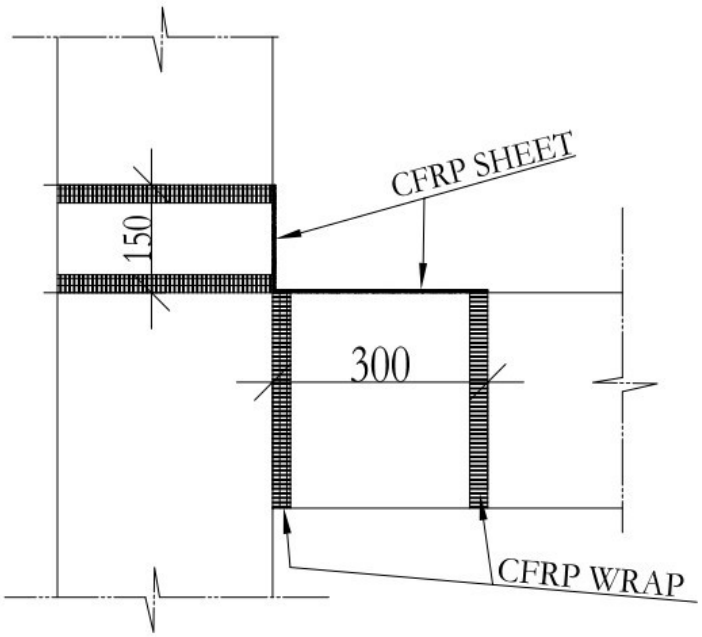

Figure 4-8: Retrofitting configuration

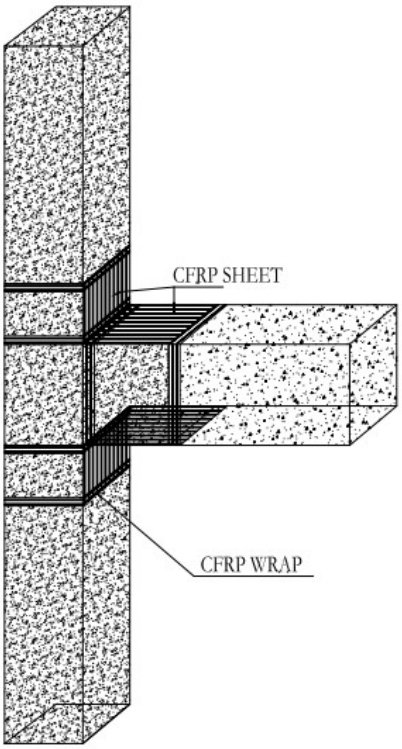

Figure 4-9: Retrofitting configuration showing CFRP fiber direction

4.6 Material properties

4.6.1 Concrete

The concrete used was obtained from Prainsa batching plant, with a targeted strength of 50MPa. 75mm diameter by 150mm height cylindrical samples as shown in Figure 33, were taken from the batch used for the BCJ specimen to conduct 21 and 28th day compressive test according to ASTM standard.

Figure 4-10: Cylinder samples taken for laboratory tests

Compressive strength of concrete

28th day compressive strength test was performed on the cured cylindrical specimen according to ASTM C39M **[42]**, using a loading rate of 0.25MPa/s. The testing equipment is shown in Figure. 4-10. For each sample cast, three -cylinder representative samples were taken and tested at 28th day. For each sampling group, average of the strength was taken, and the results tabulated in Table 4-3 below.

Figure 4-11: Testing of cylindrical samples for compressive strength.

Table 4-3: 28th day compressive strength

Specimen	28th day Compressive strength f'_c (MPa)
1	50.45
2	51.03
3	49.98
4	50.32
5	50.12
6	50.51
7	49.98
8	50.02

Stress-strain curve for one of the concrete samples tested is shown in Figure 4-11

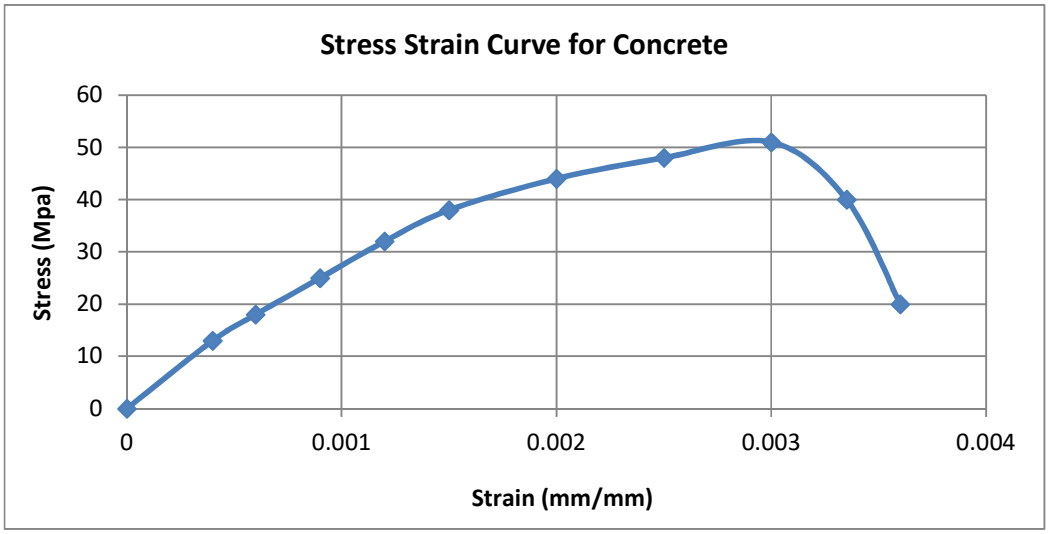

Figure 4-12: typical Stress-Strain Curve for one of the samples

Tensile strength of concrete

The tensile strength of the concrete used was obtained in the lab by conducting a direct split cylinder test on samples obtained from the Prainsa factory, (Figure 4-12).

Figure 4-13: Split cylinder test.

The test was conducted in accordance to ASTM C496 **[43]**, as shown in Figure. The average tensile strength obtained during the testing was 4.38MPa.

Elastic modulus and Poisson's ratio

In other to determine the elastic modulus of the concrete and its Poisson's ratio, ASTM C469 **[44]** was used, which requires a monotonic uniaxial compression test on the concrete cylinders in a loading frame shown in Figure 4-13. The elastic modulus was then calculated using the relation was conducted according to the relation;

$$E = (S_2 - S_1)/(\epsilon_2 - 0.000050), \qquad (4.1)$$

E is the elastic modulus, S_2 is the stress corresponding to 40-percent failure load, S_1 is the stress corresponding to ε_1 of 0.0000050. The Elastic Modulus *E* was found to be 33234MPa.

Figure 4-14: Cyclic loading test on concrete sample

The Poison's ratio is computed from this relation:

$\mu = (\varepsilon_{t2} - \varepsilon_{t1})/(\varepsilon_2$-0.000050). where ε_{t2} and ε_{t1} are transverse strains corresponding to S_2 and S_1 respectively. The Poisson's ratio obtained is 0.2.

4.6.2 Steel reinforcement

Tensile strength test was performed on samples of steel reinforcement used for the experiment at structural Mechanics lab of KFUPM in accordance to ASTM A615 **[44]**, using tensile strength machine as shown in Figure. The steel tested are of 16mm diameter and 8mm diameter for the main longitudinal reinforcement and transverse reinforcement respectively, in the beam and the column.

Figure 4-15 : Cyclic loading test on concrete sample

The stress-strain curves for the reinforcements are shown in Figures 4-15 and 4-16, with their mechanical properties given in Table 4-4.

Table 4-4 : Mechanical properties of steel reinforcements

Bar Size (mm)	Stress (MPa)		Strain (mm/mm)		Elastic Modulus (MPa)
	f_y	f_u	ε_y	ε_u	
8	580	667	0.002762	0.0105	210000
16	610	682	0.002905	0.0184	210000

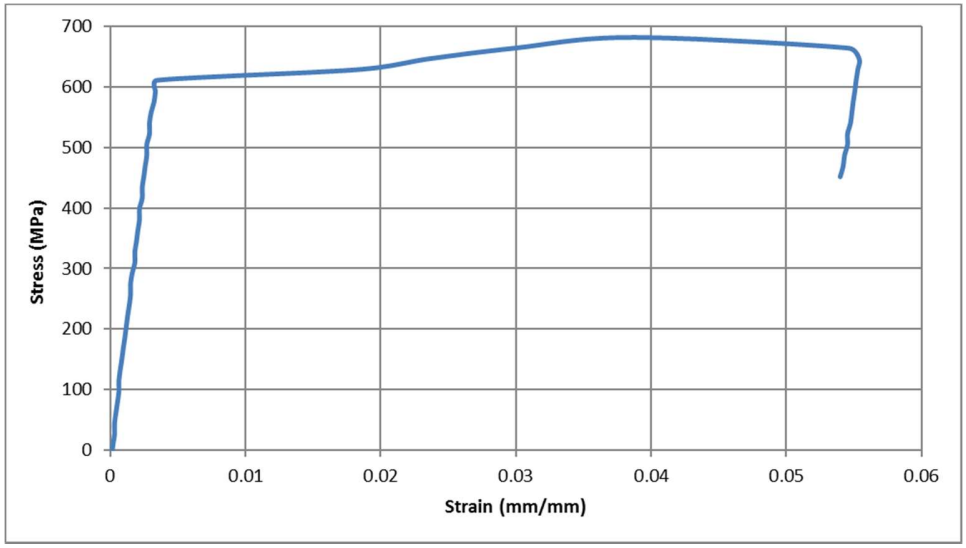

Figure 4-16: Stress-Strain Curve for 16mm- diameter bar.

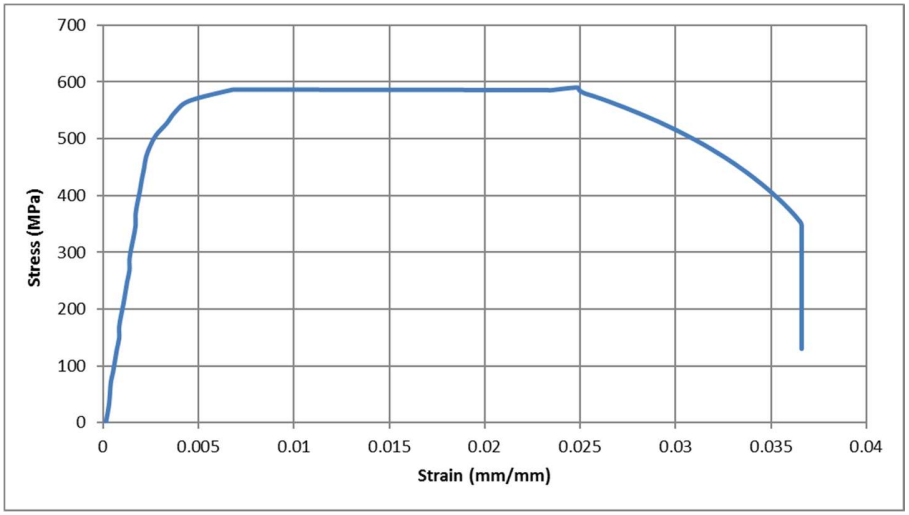

Figure 4-17: Stress-Strain curve for 8mm diameter bar.

4.6.3 CFRP retrofitting

In the retrofitting schemes, the CFRP used was obtained from a unidirectional SIKA Hex 230C bonded with high strength and high modulus epoxy- SIKADUR330. There mechanical properties were taken from the manufacturers catalogue. These properties are presented in Table 4-5.

Table 4-5: Cured properties of CFRP Hex 230C with Sikadur 330

CFRP Type	Tensile Strength (MPa)	Ultimate Strain	Tensile Modulus (GPa)	Ply thickness (mm)
Sika Hex230C	894	1.33%	65.4	0.381

The specimens tested are: control (one monotonic and one reversed cyclic), designated CSM1, and CSC1 respectively, retrofitted -one sample monotonic with 2 layers of CFRP tested under monotonic (RSM1), one sample monotonic with four layers of CFRP (RSM2), one retrofitted sample reversed cyclic, with strips of CFRP, (RSC1), one retrofitted sample with 200mm length of CFRP tested under reversed cyclic loading (RSC 2), one retrofitted sample with 300mm length of CFRP tested under reversed cyclic loading (RSC 3) and one retrofitted sample with 300mm length of CFRP for flange and web, tested under reversed cyclic loading (RSC 4). Table 4- gives a summary of all the specimens.

Table 4-6: Details of specimen tested.

S.NO	SPECIMEN DESIGNATION	TYPE OF TEST	Layers and Length of CFRP	Location of CFRP
1	CSM 1	Monotonic	N.A.	N.A.
2	CSC 1	Reversed cyclic	N.A.	N.A.
3	RSM 1	Monotonic	2L -300mm	Flange
4	RSM 2	Monotonic	4L-200mm	Flange
5	RSC 1	Reversed cyclic	1L-300mm	Web (Strips)
6	RSC 2	Reversed cyclic	2L-200mm	Flange
7	RSC 3	Reversed cyclic	2L-300mm	Flange
8	RSC 4	Reversed cyclic	2L-300mm	Flange and web

4.7 Setting up

The test setup available in the heavy structures lab of KFUPM has been designed for simulation of forces and boundary conditions that do occur during seismic action in buildings, by replicating same on the BCJ samples. A three point of inflexion that usually occur in frames subjected to lateral loads is simulated by creating a moment release at the tip of the beam, and top and bottom of the column which is similar to the BCJ cast.

In this model, the top and bottom ends of the column is restrained, while the tip load on the beam allows for load reversal that is typical in seismic loading, except for P-Δ effect, that is negligible on BCJ behavior.

The test was conducted a steel reaction loading frame with hydraulic jacks and supports.

The load was applied with the help of two hydraulic jacks; one at the column top and other at the beam tip. The jack on the column has a loading capacity of 1200 kN, while the beam tip hydraulic jack has a loading capacity of 300 kN.

The frame has a purpose built pin supports to restrain the specimens during loading conditions. Figures 4-17 and 4-18 show the schematic diagram of the frame and the BCJ specimen testing procedure.

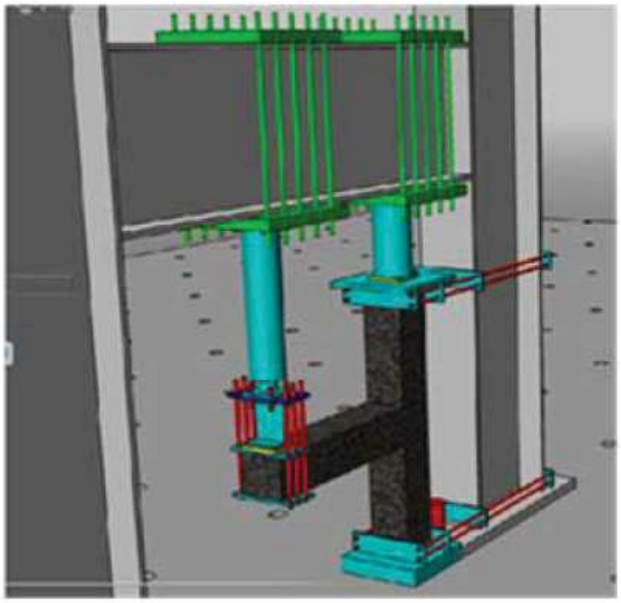

Figure 4-18 : Schematic diagram of loading frame and BCJ specimen.

Figure 4-19: A set-up for one of the BCJ specimens

4.8 Instrumentation

4.8.1 Introduction

All the specimens were designed to capture the necessary information required for the study during the specimen construction. This information includes strains in concrete and steel, beam load tip, beam tip deflection, etc. The instrumentation was done in two stage. The first stage was done in the production factory. It involves fixing of strain gauges on the steel before concreting. The second stage was done in the lab prior the test by fixing external equipment, such as LVDT's, concrete strain gauges, etc.

4.8.2 Stage one: fixing of steel strain gauges

In this stage of instrumentation, steel strain gauges of 120Ω electrical resistance capacity were fitted on the column reinforcements, beam top and bottom reinforcements, core of the BCJ. For the beams, the strain gauges were installed at the interface of the BCJ as this is that is the critical location where flexural yielding of steel will start and for the possibility of measuring the strain in the steel at which shear failure will occur. The strain gauges were installed on the column longitudinal reinforcement at the interface of the BCJ to measure the strain in the steel and the monitor the steel yielding, which will be used to determine the mode of failure of the BCJ specimen.

Critical location of the shear in the beam also had strain gauges installed to capture the load at which it will yield. Although, the beam was not designed to fail in shear. These locations are shown in Figures 4-19 and 4-20.

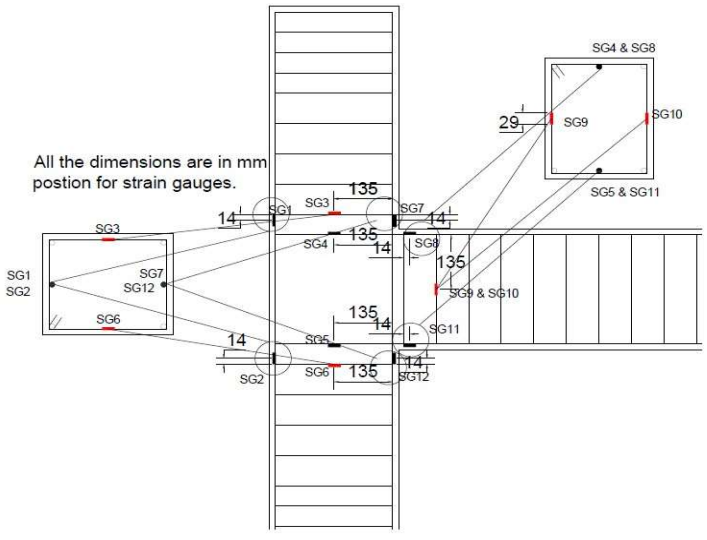

Figure 4-20: Location of strain gauges.

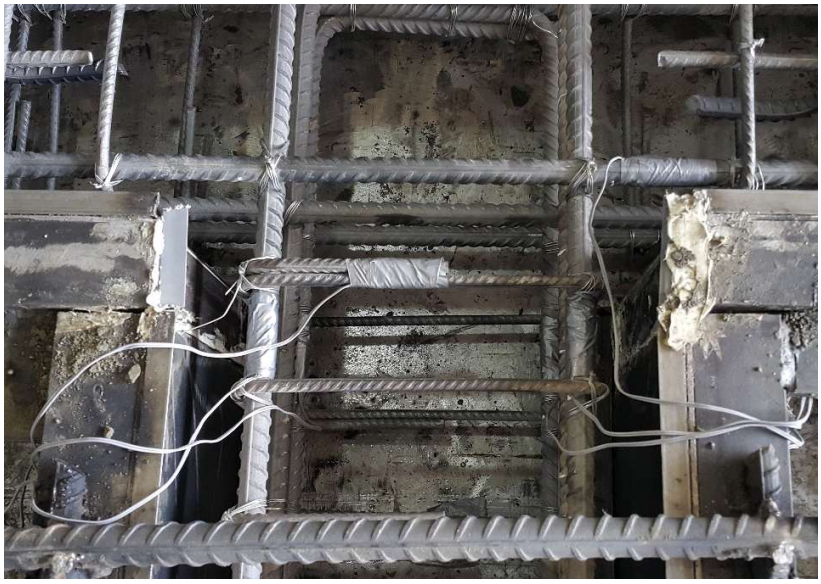

Figure 4-21: Installed strain gauges on BCJ specimen.

4.8.3 Stage two: fixing of concrete strain gauges

In this stage, installation of LVDT's, extensometer and concrete strain gauges, and CFRP strain gauges were done. LVDT's were used to monitor rotation at the point of supports, and at the core of the BCJ. Extensometer attached to the tip of the beam used to measure deflection to the nearest 0.5mm, concrete strain gauges were installed at the critical locations of the concrete (interface of the BCJ) in a vertical direction to measure the corresponding strain in the concrete at every loading step and correlate these strains with that of the steel reinforcement.

The strain gauges attached to the CFRP was used to monitor the strains in CFRP for the retrofitted specimens. A schematic diagram of the second stage of instrumentation is shown in Figures 4-21 and 4-22.

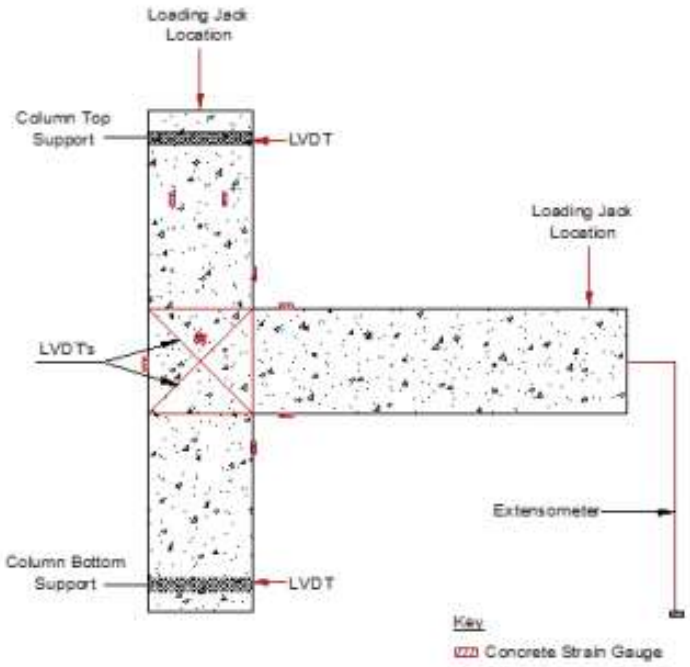

Figure 4-22: Schematic diagram of second stage of instrumentation.

Figure 4-23: BCJ specimen with external instrumentation**.**

4.9 Test program

4.9.1 Introduction

In this study, monotonic and reversed cyclic tests were performed to study the behavior of the BCJ made with high concrete compressive strength, and effect of externally flange bonded CFRP for plastic hinge relocation. Three monotonic tests were conducted, and five reversed cyclic tests were conducted in this study.

4.9.2 Monotonic loading

Three specimens (control and retrofitted) were tested under monotonic loading regime as shown in Table 4.5-4. The axial load ratio used for all the test was 0.2, corresponding to 50kN. This load was kept constant while displacement was applied to the beam tip, and the corresponding load recorded. The loading chosen was at a small increment to avoid the effect of loading rate. The BCJ was loaded until failure.

4.9.3 Reversed cyclic loading

Five specimens were tested under reversed cyclic loading regime, using displacement controlled. The reversed cyclic loading test was used to simulate actual seismic incidence that do occur in real life for BCJ of building frames. The axial load on the column was kept as was in the monotonic test, which is 150kN. The loading was applied using loading

protocol calculated and shown in Table 4-7 and Figure 4-23. The loading was applied up till ultimate failure in the BCJ specimen. The same loading protocol was applied for all of the specimens marked for reversed cyclic loading test. The drift ratio percentage was calculated from the relation:

Drift ratio percentage $= (beam\ tip\ displacement / beam\ length)\ x\ 100\%$.

Table 4-7: Loading protocol for reversed cyclic test.

Cycle	Drift ratio (%)	Push (mm)	Pull (mm)
1	0.11	1	-1
2	0.22	2	-2
3	0.33	3	-3
4	0.44	4	-4
5	0.56	5	-5
6	0.67	6	-6
7	0.78	7	-7
8	0.89	8	-8
9	1.00	9	-9
10	1.11	10	-10
11	1.22	11	-11
12	1.33	12	-12
13	1.44	13	-13
14	1.56	14	-14
15	1.67	15	-15
16	1.78	16	-16
17	1.89	17	-17
18	2.00	18	-18
19	2.11	19	-19
20	2.22	20	-20
21	2.33	21	-21
22	2.44	22	-22
23	2.56	23	-23
24	2.67	24	-24
25	2.78	25	-25
26	2.89	26	-26
27	3.00	27	-27
28	3.11	28	-28

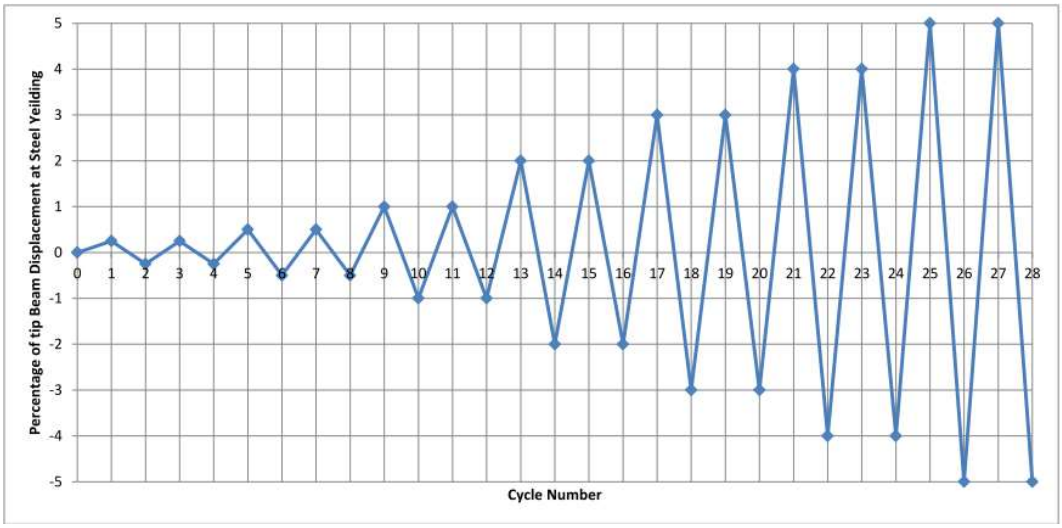

Figure 4-24: Loading protocol chart for reversed cyclic tests.

CHAPTER 5

EXPERIMENTAL RESULTS AND DISCUSSIONS

5.1 Introduction

This chapter discusses the outcomes of the experimental program as previously described in chapter four. As the major aim of the experiment is to investigate the behavior of BCJ made with high compressive strength under seismic loading, and the retrofitting of such BCJ using externally flange bonded CFRP. The parameters to be discussed and monitored are mode of failure, crack pattern and its propagation, load-displacement curve, and ductility. Those parameters will be recorded and compared with retrofitted samples.

5.2 Performance of BCJ under monotonic loading

5.2.1 Control specimen monotonic loading (CSM 1)

This specimen was tested under monotonic loading with ALR of 0.2, corresponding to 150kN. The first crack was observed at a load of 36.1kN corresponding to a beam tip displacement of 2.0mm. this first crack occurred at the interface of the BCJ, which is the

critical location for flexural behavior. The cracks became wider as the test progressed, with other flexural cracks developed in other region of the beam. The steel yielded at a load of 103kN, and this yield penetrates the core of the BCJ, and further lead to fine hair shear crack. As the test continue, the shear crack did not grow, but the flexural crack (at the interface of the BCJ) became wider and dominant.

The extensometer to monitor the displacement got damaged during test and made it impossible to measure the displacement. The test continued up to ultimate failure of the sample, and the crack at the BCJ interface was the major plastic hinge that formed in the BCJ. The ultimate damage mode for the specimen and the load displacement curve are shown in Figures 5-1 and 5-2.

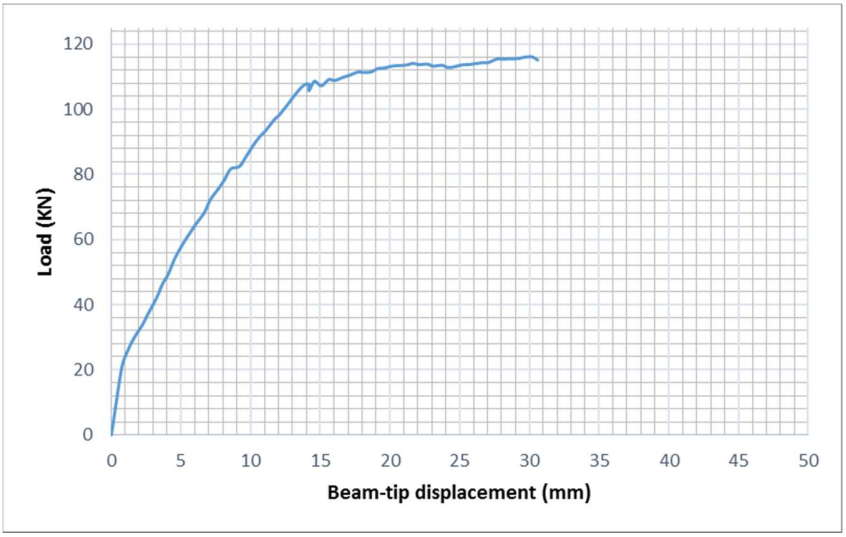

Figure 5-1 : Load displacement curve for CSM

Figure 5-2: Failure of CSM at ultimate load.

The strain in the column beam top reinforcement was 0.00398mm/mm which shows the failure mode is BCJ initiated by the flexural yielding of the beam top reinforcement.

5.2.2 Retrofitted specimen monotonic 1 (RSM 1).

This specimen was retrofitted with two layers of CFRP of 300mm length, and tested under monotonic loading. The first crack was observed at a load of 38kN corresponding to a beam tip displacement of 2.4mm. This first crack occurred at the termination end of CFRP bonded on the beam.

The crack became wider as the test progressed, with other flexural cracks developed in other region of the beam, but were all flexural in nature. The steel yielded at a load of

110kN, and this yield penetrates the core of the BCJ, and further lead to fine hair shear crack. As the test continue, the shear crack did not grow, but the flexural crack after the CFRP became wider and dominant.

The relocation of the plastic hinge is as a result of the addition of CFRP which act as external reinforcement and increase the beam capacity within the length of the CFRP.

The specimen reached its ultimate capacity at a load of 144kN, as against 125kN for the CSM. Comparison of the strains in the beam top reinforcement showed that the BCJ failed by BCJ as a result of the yielding of the reinforcement. The strain in the CFRP did not reach its ultimate strain to cause rupture. The CFRP failure by debonding from the concrete cover.

The ultimate damage mode for the specimen and the load displacement curve are shown in Figures 5-3 and 5-4.

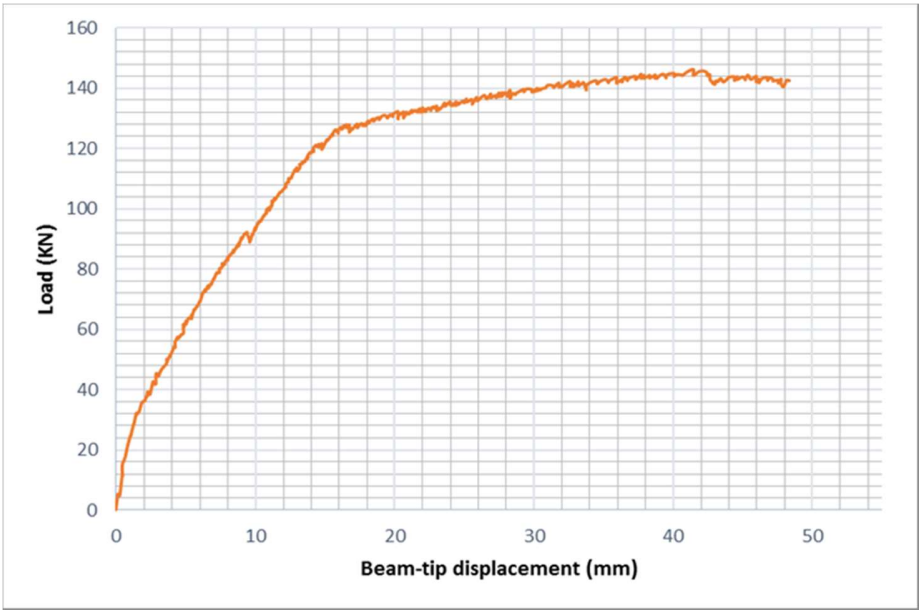

Figure 5-3: Load displacement curve for RSM 1

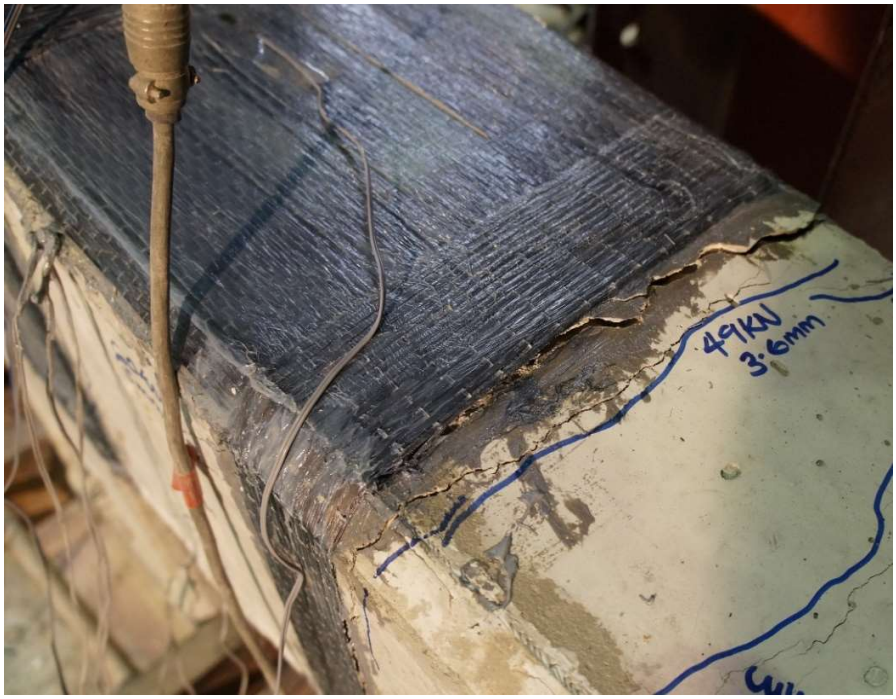

Figure 5-4: Failure mode of RSM 1

5.2.3 Retrofitted specimen monotonic 2 (RSM 2)

In this specimen, four layers of CFRP of 200mm length was used. The specimen was tested under monotonic loading. The first crack was observed at a load of 42kN corresponding to a beam tip displacement of 3.1mm. This first crack occurred at the termination end of CFRP bonded on the beam as shown in Figure 5-5.

The crack became wider as the test progressed, with other flexural cracks developed in other region of the beam, but were all flexural in nature. The beam top reinforcement yielded at a load of 114kN, and this yield penetrates the core of the BCJ, and further lead to fine hair shear crack. As the test continue, the shear crack did not grow, but the flexural crack after the CFRP became wider and dominant.

The specimen reached ultimate capacity at a load of 132kN. It was noticed that this specimen had a higher ductility than RSM 1. The strain in the CFRP did not reach its ultimate strain to cause rupture. The CFRP failed by debonding from the concrete cover. The ultimate damage mode for the specimen is shown in Figure 5-6.

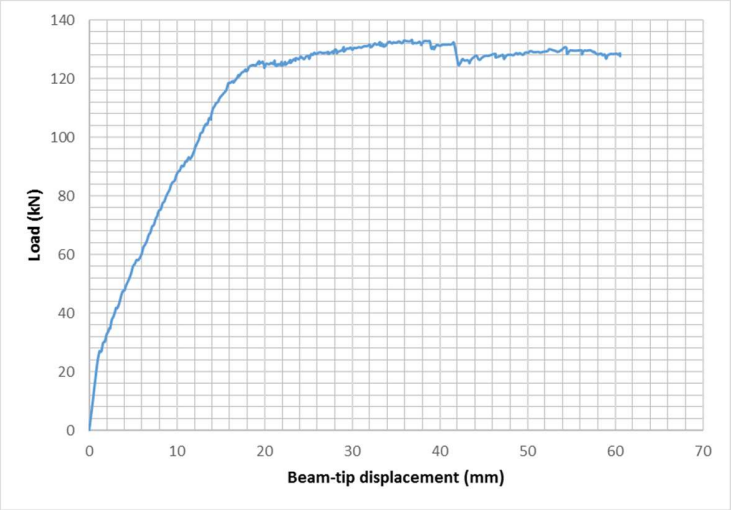

Figure 5-5: Load-displacement curve for RSM 2

Figure 5-6: Failure mode of RSM 2.

5.3 Performance of specimens under reversed cyclic load

5.3.1 Control specimen cyclic (CSC)

This specimen was tested under reversed cyclic loading using displacement controlled regime. The first crack was observed at a load of 37.1kN corresponding to a beam tip displacement of 2.5mm in the push direction 32kN in the pull direction. This crack occurred at the interface of the BCJ.

The cracks became wider as the test progressed, and the top steel yielded at a load of 103kN, while the bottom steel yielded at a load of 101kN. The yielding penetrates the core of the BCJ, and led to shear crack in the core of the BCJ. As the test continue, the shear crack grew, but the flexural crack (at the interface of the BCJ) became wider and dominant. the specimen could not take additional load when the shear crack became wider, due to softening of the concrete.

The ultimate damage mode for the specimen and the load displacement curve are shown in Figures 5.7-5-9.

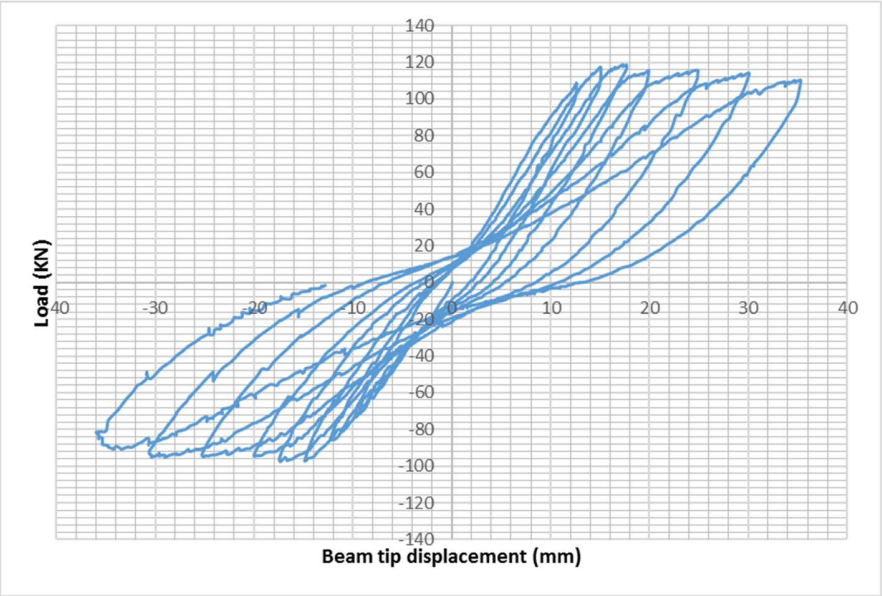

Figure 5-7: Hysteresis curve for CSC

Figure 5-8: Damage pattern of CSC.

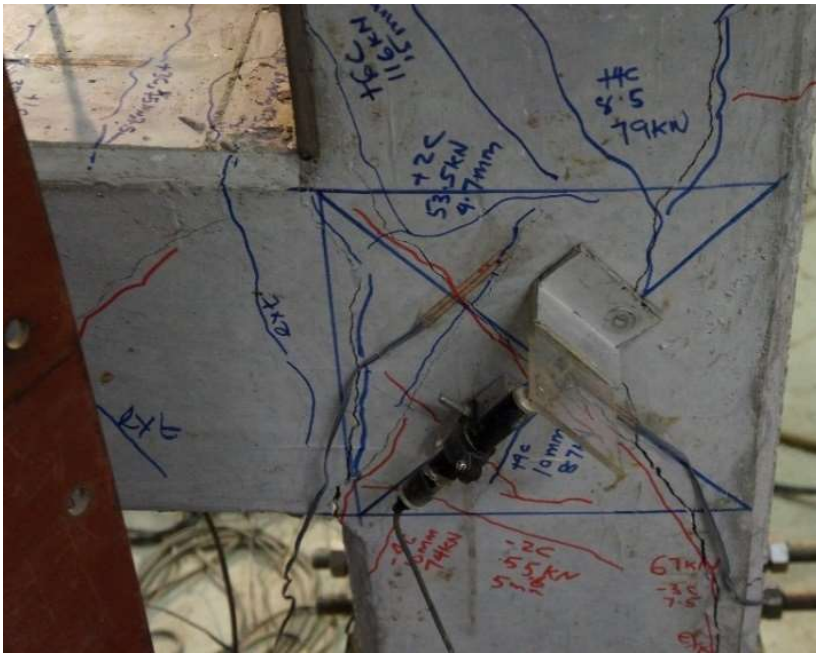

Figure 5-9: crack pattern of CSC.

5.3.2 Retrofitted specimen cyclic 1 (RSC 1)

In this specimen, one layer of 300mm length by 50mm width CFRP strips was bonded to the web of the beam and tested under reversed cyclic loading using displacement controlled regime. The first crack was observed at a load of 37.5kN corresponding to a beam tip displacement of 2.5mm in the push direction 33kN in the pull direction. The crack occurred at the interface of the BCJ.

During the test, the crack became wider. The top steel yielded at a load of 107kN, while the bottom steel yielded at a load of 101kN. Fine hair shear crack was noticed at in the core of the BCJ, but could not grow due to CFRP bonded around the joint, which act as external reinforcement for the joint. As the test continue, the flexural crack (at the interface of the BCJ) became wider and the CFRP in this region ruptures as the strain in the CFRP when

measured was 0.0142, which is higher than its ultimate rupture strain. This rupture led to the failure of the sample by flexure with the plastic hinge formed at the interface of the BCJ. When compared to the CSC, the RSC 1 had a higher ductility as shown in Figures 5.3-1.

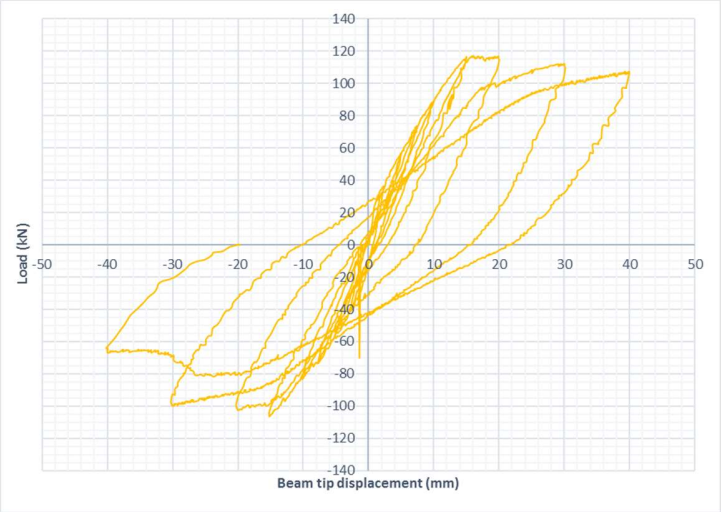

Figure 5-10 : Hysteresis curve for RSC 1

Figure 5-11: Failure of RSC1**.**

5.3.3 Retrofitted specimen cyclic 2 (RSC 2)

In this specimen, two layers of 200mm length CFRP covering the entire width of the beam was bonded to the flange of the beam and tested under reversed cyclic loading using displacement controlled regime. The first crack was observed at a load of 38kN corresponding to a beam tip displacement of 2.5mm in the push direction 35kN in the pull direction. The crack occurred at the termination length of the CFRP on the BCJ.

During the test, the crack became wider. The top steel yielded at a load of 120kN, while the bottom steel yielded at a load of 111kN. Fine hair shear crack was noticed at in the core of the BCJ, but did not extend beyond the hairline. As the test progress, another flexural crack occurred at the interface of the BCJ, but did not grow as compared to that at the termination of the CFRP. The strain in CFRP was 0.00125 which is much less that its rupture strain. The CFRP failed by debonding. The plastic hinge formed after the CFRP termination length was a great success, as it is the aim of the experiment. The load displacement curve and failure mode is shown in Figure 5-12 - 5- 13.

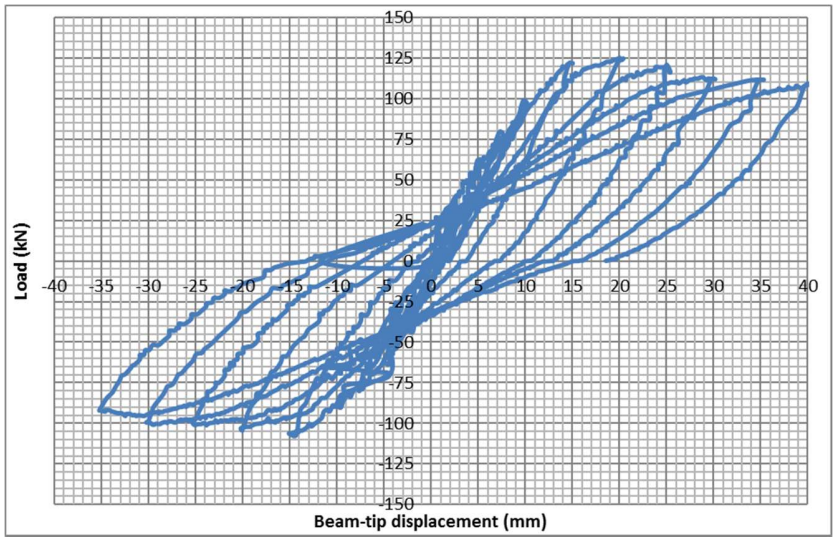

Figure 5-12: RSC 2 hysteresis curve

Figure 5-13: RSC mode of failure.

5.3.4 Retrofitted specimen cyclic 3 (RSC 3)

In this specimen, two layers of 300mm length CFRP covering the entire width of the beam was bonded to the flange of the beam and tested under reversed cyclic loading using

displacement controlled regime. The first crack was observed at a load of 36kN corresponding to a beam tip displacement of 2.3mm in the push direction 33kN in the pull direction. The crack occurred at the termination length of the CFRP on the BCJ.

The top steel yielded at a load of 115kN, while the bottom steel yielded at a load of 108kN. Fine hair shear crack was noticed at in the core of the BCJAs the test progress, another flexural crack occurred at the interface of the BCJ, but did not grow as compared to that at the termination of the CFRP. The strain in CFRP was 0.00121 which is much less that its rupture strain. The CFRP failed by debonding. The load displacement curve and failure mode is shown in Figure 5-14 – 5-15.

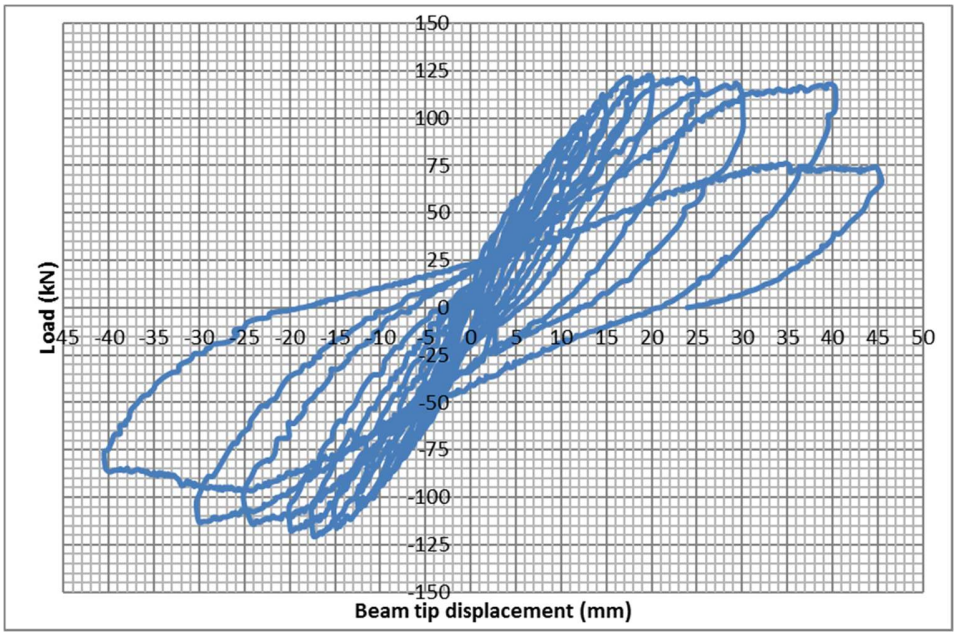

Figure 5-14: hysteresis curve

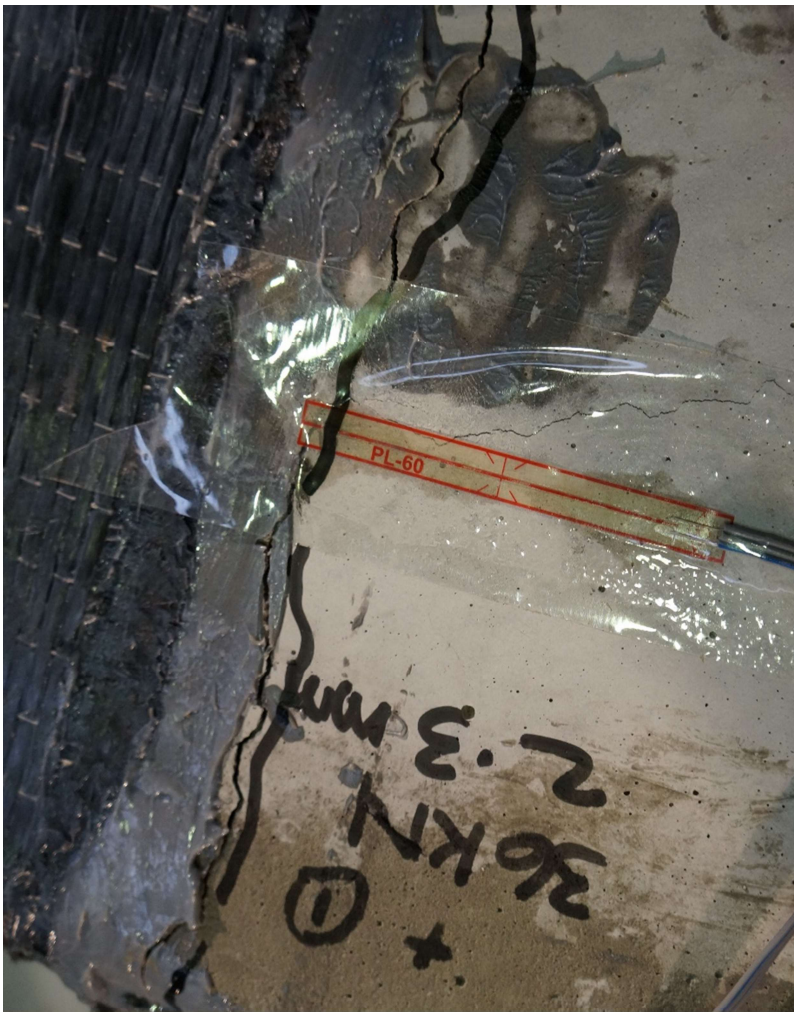

Figure 5-15: location of plastic hinge

5.3.5 Retrofitted specimen cyclic 4 (RSC 4)

In this specimen, two layers of 300mm length CFRP covering the entire width of the beam was bonded to the flange and web of the beam. The RSC 4 was tested under reversed cyclic loading using displacement controlled regime. The first crack was observed at a load of 36.3kN corresponding to a beam tip displacement of 2.7mm in the push direction 33kN in the pull direction. The first crack occurred at the termination length of the CFRP on the BCJ.

The top steel yielded at a load of 119kN, while the bottom steel yielded at a load of 108kN. Fine hair shear crack was noticed at in the core of the BCJ, but did not extend beyond the hairline. As the test progress, another flexural crack occurred at the interface of the BCJ, but did not grow as compared to that at the termination of the CFRP. The strain in CFRP was 0.00115 which is much less that its rupture strain. The CFRP failed by debonding, and the beam failure by flexure-shear as shown in Figure 5-16 – 5-17.

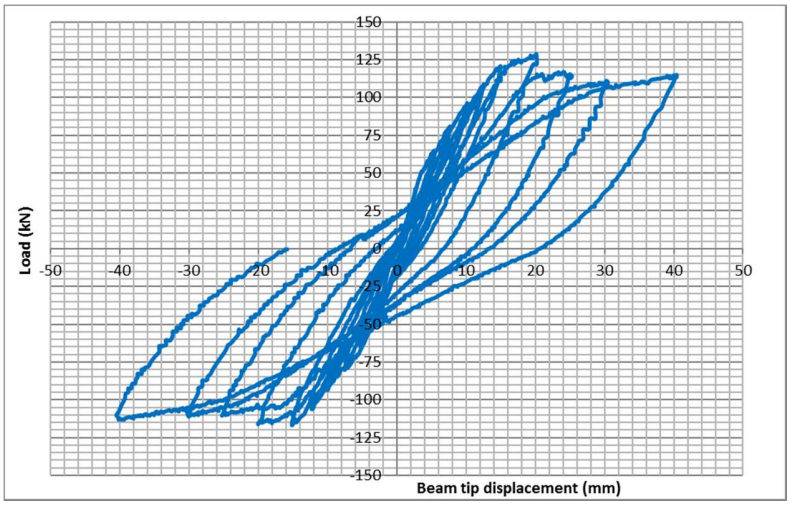

Figure 5-16: Hysteresis curve

Figure 5-17: plastic hinge location

5.4 Summary of experimental results

From the results presented above, it is noted that BCJ made with high strength concrete can fail in flexure with plastic hinge formation at the interface of the BCJ as against shear failure. This location of plastic hinge is not desirable because of the penetration of the yield into the core of the BCJ which can damage the bond between the steel longitudinal reinforcement and the concrete, and further leads to shear failure.

Shear failure is a global failure which is also not desirable, flexural failure is a local failure preferable in reinforced concrete building during seismic action. The application of CFRP on the flange of the beam, relocated the plastic hinge from the interface of the BCJ to a distance inside the beam.

All the retrofitted specimens tested showed improved ductility and load carrying capacity as a result of relocating the plastic hinge away from the BCJ interface.

CHAPTER 6

NUMERICAL MODELLING OF BCJ

6.1 Introduction

In this chapter, numerical modeling of the experimentally tested BCJ is simulated. Different approaches of simulation are discussed as regards the nonlinear behavior of concrete under loading and the associated challenges involve using a commercially available FE element software- ABAQUS. The numerical modeling will be used to validate the experimental results obtained. Such validation will provide a better understanding to the results obtained experimentally.

6.2 Finite Element Modelling

Finite element modeling used in this study focus on modeling of concrete, steel reinforcement, CFRP, epoxy and the interaction between the various elements. Dynamic explicit solver analysis was used to solve convergence problem that do occur in reinforced concrete element modelling

6.3 Damage models available in Abaqus

ABAQUS (2013) is a commercially available nonlinear finite element used to simulate and validate different experimental load testing on RC structures and steel structures. It requires materials constitutive and experimental data as input files for it to initiate the analysis. Of the many available concrete damage models in ABAQUS such as smeared crack concrete model, brittle crack concrete model, etc., the concrete damage plasticity (CDP) was chosen, because it has the capability to simulate the elastic and inelastic behavior of concrete in tension and compression with different yield stress as observed in the laboratory. The CDP was proposed by Lubliner et al. **[45]** and later improved by Lee et- al. **[46]**. The model uses a yield surface for its failure criterion by combining Drucker-Prager with Rankine.

6.3.1 Concrete models

The concrete damage plasticity available in Abaqus requires the definition of:

1. Uniaxial compressive and tensile stress-strain relation for the concrete
2. Compressive and tensile damage parameters for the concrete.

The fib concrete model was selected because it possesses advanced parameters for controlling post-peak behavior of the stress-strain properties of the concrete. The stress-strain curve of this model is shown in Figure 6-1.

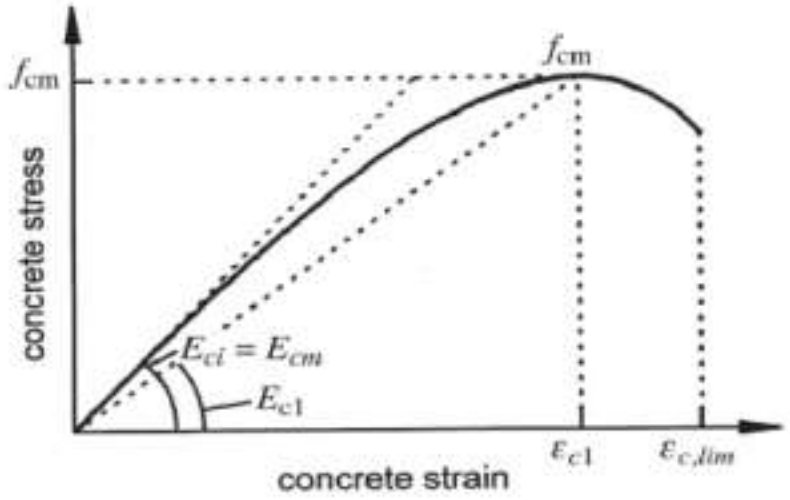

Figure 6-1: stress-strain curve for Fib (2003) concrete model

In using this model, the bilinear properties of the concrete must be determined for accurate prediction of the crack and damage modes of the concrete. The damage parameters for compression, d_c and tension, d_t are obtained by performing numerical integration of the area under the uniaxial compression and tension curve shown in Figures 6-2 and 6-3. The compression damage parameter d_c obtained from the numerical integration of the curve can be expressed as

$$d_c = 1 - \frac{\sigma_c {E_c}^{-1}}{{\epsilon_c}^{pl}\left(\frac{1}{b_c} - 1\right) + \sigma_c {E_c}^{-1}} \qquad (6.1)$$

σ_c is the compressive stress of the concrete, E_c is the elastic modulus, ${\epsilon_c}^{pl}$ is the plastic strain at corresponding to the compressive stress, and b_c is a constant which ranges between 0 and 1, that is $0 < b_c < 1$.

Similarly, the tension damage parameter d_t can be obtained from the relation;

$$d_t = 1 - \frac{\sigma_t {E_c}^{-1}}{{\epsilon_t}^{pl}\left(\frac{1}{b_t}-1\right)+\sigma_t {E_c}^{-1}} \tag{6.2}$$

σ_t is the tensile stress of the concrete, E_c is the elastic modulus, ${\epsilon_t}^{pl}$ is the plastic strain at corresponding to the tensile stress, and b_t is a constant which ranges between 0 and 1, that is $0 < b_t < 1$.

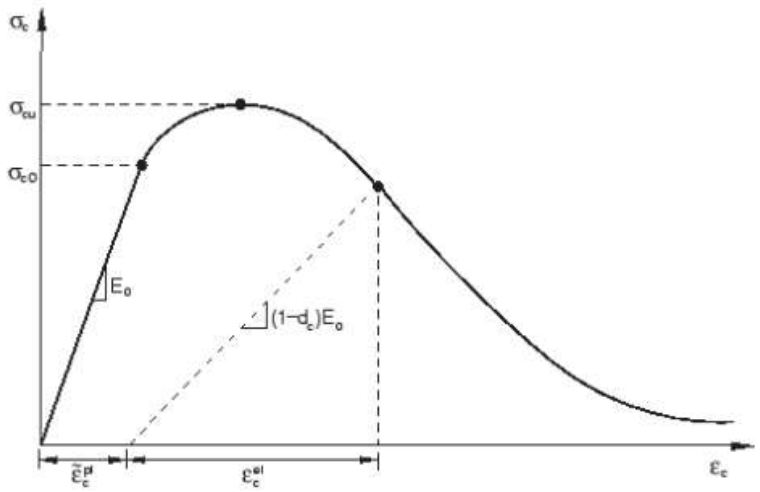

Figure 6-2: Uniaxial compressive stress-strain curve

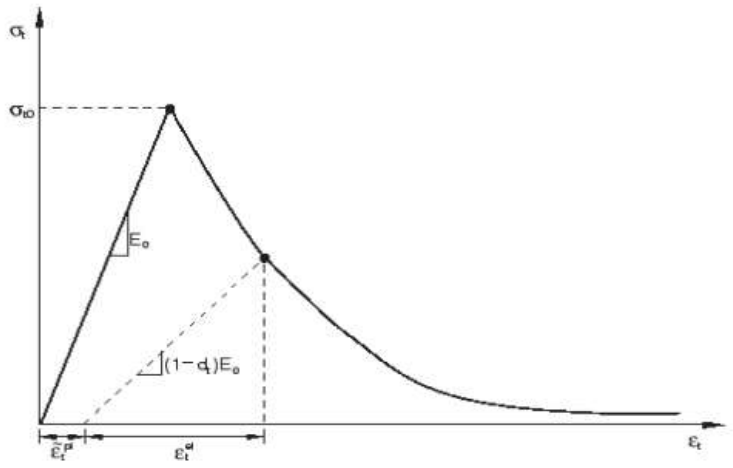

Figure 6-3: Uniaxial tensile stress-strain curve for tension damage parameter.

The CDP chosen for this study requires the definition of Poisson's and dilatation angle in other to capture the inelastic behavior of the concrete. The Poisson's ratio is the governing factor for the change in volume of concrete below its critical stress level. Once this critical stress level is reached, the plastic volume of the concrete increases under stress. The governing factor for this increase in plastic volume is the dilatation angle.

The Poisson's ratio can be easily determined in the laboratory, while the dilatation angle is difficult to obtain. The dilatation angle is therefore obtained from literature. Table 6-1 summarizes the values used for the CDP in ABAQUS.

Table 6-1: CDP for plastic damage in concrete used in Abaqus.

Strength of concrete (MPa)	Mass density (tonne/mm3)	Elastic modulus (MPa)	Poisson's ratio	Angle of dilatancy (degrees)	Eccentricity	f_{bo}/f_{co}
50	2.4E-009	33234	0.2	36	0.1	1.16

6.3.2 Modelling of steel reinforcement

The steel reinforcement (longitudinal and transverse) was modeled as a truss element embedded in concrete assuming a perfect bonding between the steel and concrete, using embedment technique.

If truss element is used for steel reinforcement, it is unnecessary to consider the complex behavior of steel when subjected to multi-axial stresses. Therefore, a perfect elasto-plastic

is used to idealize the stress-curve under tension and/or compression. Table 6-2 summarizes the values used for the steel reinforcement.

Table 6-2: Mechanical properties of steel used in FE modelling.

Yield strength (MPa)	Mass density (tonne/mm3)	Elastic modulus (MPa)	Poisson's ratio
610	7.85E-009	210000	0.3

6.3.3 CFRP modelling

The behavior of FRPs depend on their mechanical properties, fiber orientation, length, shape and constituent fibers, properties of the epoxy adhesive, and nature of the surface to which they are bonded. FRPs usually display linear elastic property until failure without any inelastic deformation. There are many proposed theories to represent the orthotropic plane stress failure of FRPs.

The Tsai-Wu theory was used to simulate the failure surface of CFRP in the ABAQUS program because it is suitable for unidirectional FRP as compared to the Tsai-Hill's criterion as it accounts for Bausch Inger's effect. Tensile values were taken as positive, while compressive taken as negative so as to account for FRPs behavior in both tension and compression as required in Tsai-Wu theory. Cohesive zone model (CZM) was adopted by using the traction-separation law.

The epoxy was bonded to the concrete surface using tied to ensure that nodes on the interface of the epoxy have the same displacement as nodes on the concrete interface. By

doing this, normal and shear stresses along the concrete epoxy-interface would have been accounted for.

It has been reported that the contact element is not a key factor for predicting behavior of the FRP-concrete bond, but the fracture energy of the concrete-epoxy interface plays an important role in the results of such prediction.

6.4 Calibration and FE validation of experimental results

The material properties obtained in the laboratory for concrete, steel reinforcement, and CFRP were used to calibrate a model of BCJ by choosing the appropriate mesh size, termination time and time step as required for all FE simulations.

The samples tested experimentally were done validated using the calibrated model so as to getting a better information and understanding of the experimental results. These results are then compared and contrasted as discussed below.

6.4.1 Validation of CSM

The FE model results for this specimen was in agreement with the experimental results in terms of load capacity, strains, failure mode, and steel reinforcement yielding. As seen in Figure 6-4, the load-displacement had approximate same slope both in the elastic and inelastic range.

The maximum load predicted by the experiment is 115kN, while the finite element predicted 114.8kN. The damage pattern of the experimental and FE are shown in Figures

6-5 and 6-6. The specimen failed in flexure as shown. The maximum strains in the two were also matched. The experiment had a maximum strain of 0.002901 mm/mm while the FE model had 0.002904 as shown in Figure

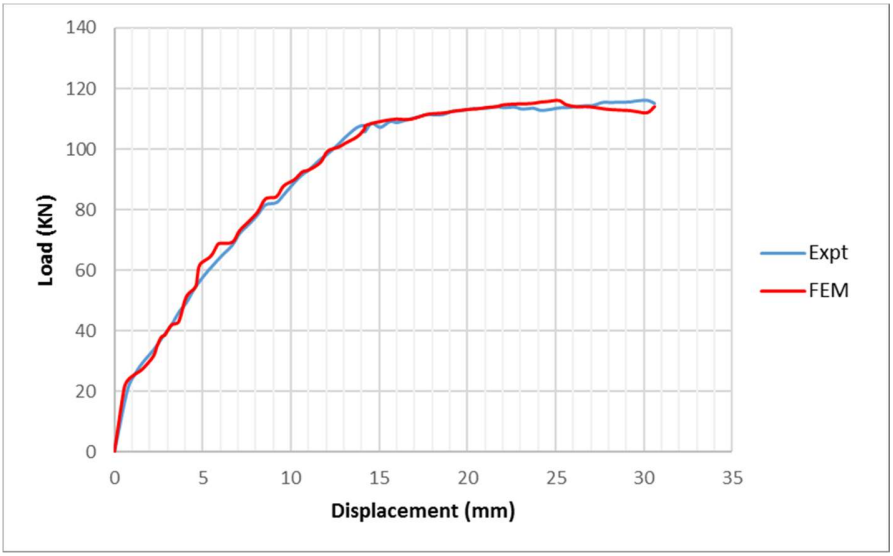

Figure 6-4: Load displacement curve for CSM (Expt. & FEM)

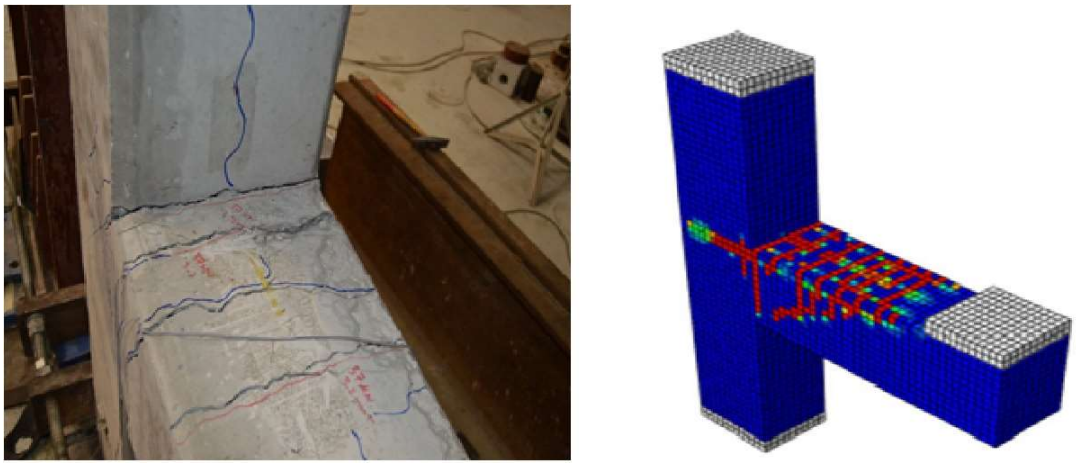

Figure 6-5: Comparison of damage pattern of Expt. And FEM

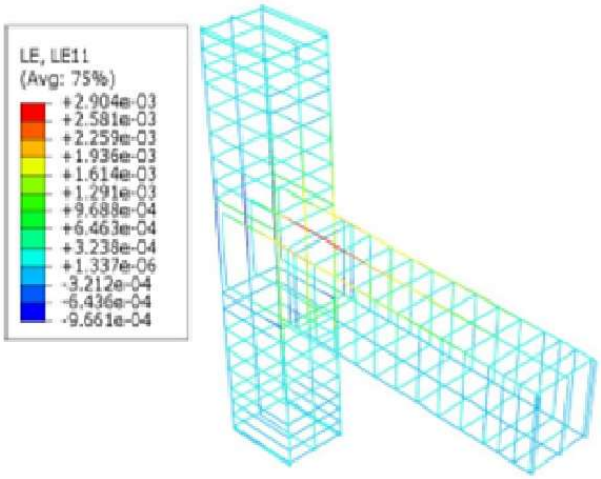

Figure 6-6: Strain in steel reinforcement (FEM)

6.4.2 Validation of RSM 1

For this retrofitted specimen having 300mm bonded length of CFRP compared with the experimental result, the load-displacement is shown in Figure 6-7. The maximum load predicted by the experiment is 140kN, while the finite element predicted 144.3kN. The damage pattern of the experimental and FE are shown in Figure 6-8.

The maximum strains in the steel reinforcement for the two were also matched. The experiment had a maximum strain of 0.002701 mm/mm while the FE model had 0.002874 as shown in Figure 6-9. The strain in the steel reinforcement for the retrofitted specimen because of CFRP which takes part of the load as additional external reinforcement.

The CFRP maximum strain from the experiment was 0.00958mm/mm, while that of the FE was 0.009656mm/mm. These values are far less than the ultimate strain for rupture in the CFRP. The maximum strain of the epoxy used was 0.9% (0.0090mm/mm) which is less than that in the CFRP and in both FE and the experiment.

This accounts for debonding failure of the CFRP noticed during the experiment.

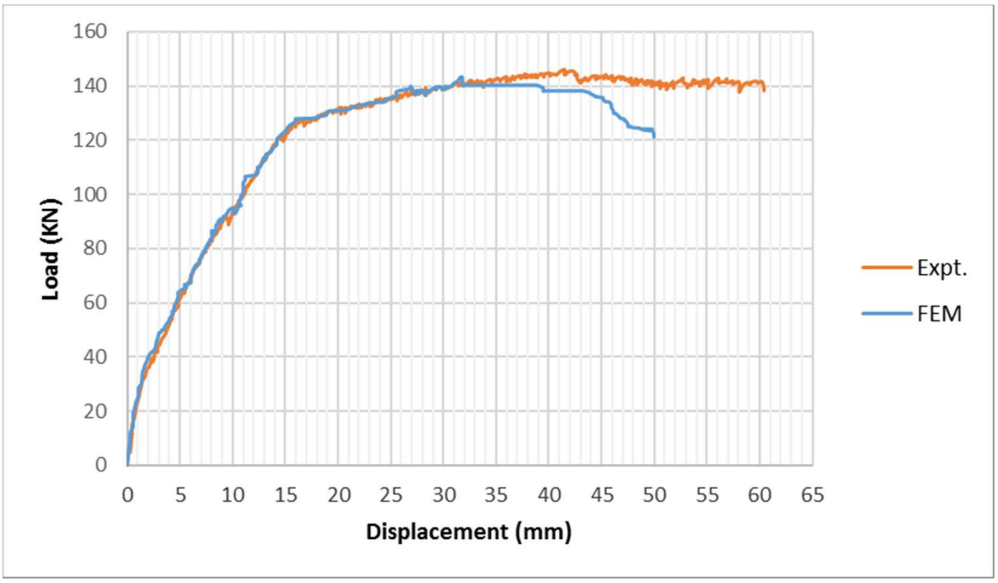

Figure 6-7: Load displacement curve for RSM (Expt. & FEM)

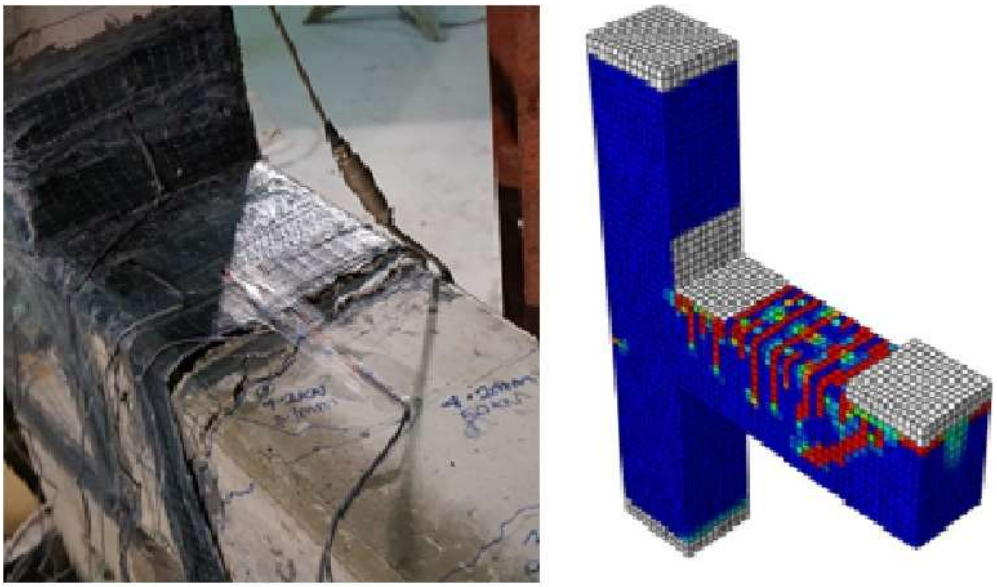

Figure 6-8: Comparison of damage pattern of Expt. And FEM (RSM)

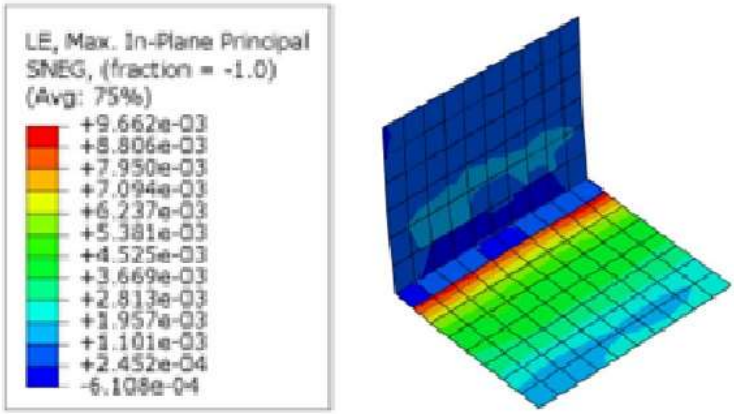

Figure 6-9: Strain in CFRP for RSM 1.

CHAPTER 7

MECHANISTIC MODEL FOR PREDICTING

FLEXURAL CAPACITY OF BEAM COLUMN JOINT

7.1 Introduction

In this chapter, mechanistic model used in predicting the strength of CFRP retrofitted structures are discussed and analyzed. While many works have been conducted and published for shear strengthening, models for flexural strengthening are not readily available in literature.

As a result, the ACI 440 which is semi-empirical will be used for the flexural strengthening. The ACI 440 code will be used to match the strains in the CFRP and validate the enhanced capacity of the beam after retrofitting.

7.2 Development of moment capacity equation

The moment capacity of the beam is directly related to the joint shear stress. The moment capacity of the retrofitted BCJ is the sum of the moment capacity of the original specimen and the contribution of CFRP; that is,

$$M_{n,retr} = M_n + M_{cfrp} \qquad (7.1)$$

Where $M_{n,retr}$ is the flexural strength contributed by the steel and CFRP, which can be obtained from section analysis, M_n is the flexural strength of the specimen due to steel alone, and M_{cfrp} is the flexural strength contribution of CFRP.

$$M_{cfrp} = T_{cfrp} d_{frp} \quad (7.2)$$

$$T_{cfrp} = \varepsilon_{cfrp} A_{cfrp} E_{cfrp} \quad (7.3)$$

$$A_{cfrp} = n_{cfrp} t_{cfrp} b_{cfrp} \quad (7.4)$$

The critical parameter in the above equations is the ε_{cfrp} (maximum allowable strain in the CFRP), which depends on the preferred mode of failure of the retrofitted specimen. ACI 440, grouped the failure mode into the following:

1. Concrete crushing in compression before steel yielding;
2. Steel yielding in tension proceeded by rupture of CFRP;
3. Steel yielding in tension proceeded by concrete crushing in compression;
4. Delamination of concrete cover in shear or tension; and
5. Debonding of the CFRP from the concrete substrate.

CFRP rupture is a brittle mode of failure which is not desirable in concrete design and must be avoided. In most cases, CFRP do not get to the strains that will cause rupture, before the epoxy fails. This failure of epoxy in tension usually lead to debonding failure mode, and this is the mode of failure selected as observed during the experimental procedures.

The maximum allowable strain in the CFRP (ε_{cfrp}), is then limited to the strain at which debonding will occur, which is given by:

$$\varepsilon_{fd} = 0.41\sqrt{\frac{f_c'}{nE_{cfrp}t_{cfrp}}} \leq 0.9\varepsilon_{fu}; \quad (7.5)$$

The stress-block for the retrofitted beam is shown in Figure 7-1.

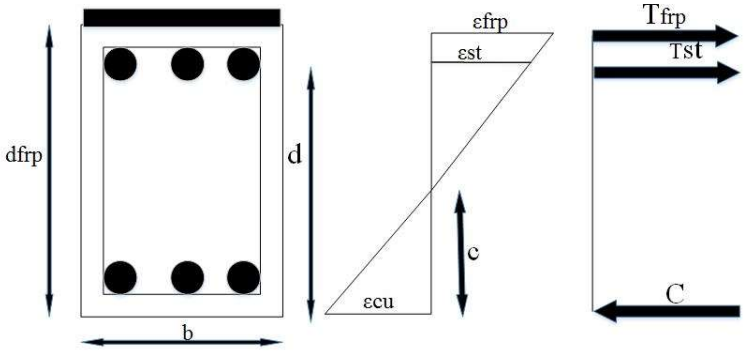

Figure 7-1: Stress block diagram for section analysis

For section equilibrium,

$$T_{cfrp} + T_{st} = C \quad (7.6)$$

neglecting the contribution of bottom steel, where C is the compressive force of the concrete, and T_{st} is the tensile force in the beam longitudinal reinforcement.

$$C = \alpha_1 f_c' A_c, \quad (7.7)$$

$$T_{st} = \alpha f_y A_{st} \quad (7.8)$$

α is taken as 1.25, to account strain hardening, while α_1 depends on the grade of concrete.

The determination of equilibrium equation depends on the value of "c" (Figure 6-1), which is usually an iterative process because the strain in the steel depends on the stress level either the steel has yielded or not. The equilibrium equation has three unknowns which is difficult to solve.

In other to solve for c, the strain in the CFRP is taken as debonding strain. Using RSM 2 as an example, and solving for the depth of the concrete block "c", gives 46.93mm, and $f_s = f_y$. The moment capacity with the steel alone (M_{ns}) was 89.1kNm, while that contributed by the CFRP ($M_{n,cfrp}$) was 59.3kNm, hence, $\emptyset M_{n,retro}$ became 125.5kNm corresponding to a beam tip load of 139.4kN, as against 132kN observed during the experiment. The corresponding strain in the CFRP measured experimentally was 0.00882mm/mm, while predicted was 0.0091mm/mm.

The shear capacity of the original BCJ is given by

$$V_{jh} = T_{st} - V_c; \tag{7.9}$$

$$V_c = \frac{P_n(L+0.5h_c)}{H} \tag{7.10}$$

After retrofitting,

$$V_{jh,retr} = T_{st} + T_{cfrp} - V_c \tag{7.11}$$

The joint shear strength which consider all the various parameters influencing the strength of the BCJ without CFRP and transverse reinforcement in the joint as proposed by Tsonos **[46]** is:

$$V_n = 0.525A_j(f_c')^{2/3} \tag{7.12}$$

If there was no shear failure before retrofitting, it is then necessary to ensure that shear failure will not occur in the specimen after retrofitting. Therefore, the joint shear demand after retrofitting must be less than the joint shear strength of the original specimen as expressed in equation (7.13)

$$\left(0.525A_j(f_c')^{2/3}\right) \gg (T_{st} + T_{cfrp} - V_c) \quad (7.13)$$

7.3 Validation of modeled equation

During the experiment, none of the retrofitted specimens failed in shear, even though hairline shear cracks were observed. It is therefore necessary to verify the validity of equation (7.13).

For the case of RSM 2, $P_n = 118.8kN$ ($by\ dividing$ 132 by 0.9), $T_{cfrp} = 209.2kN$, $T_{st} = 460kN$, computing V_c from equation (7.10) gives 89.1kN, and $V_n = 534.4kN$ computed from equation (7.12).

Equation (7.13) becomes:

$$(534.4\text{kN}) \gg (526.1\text{kN})$$

As seen above, the joint shear demand and shear strength capacity are only slightly difference by a value of 8.3kN, which is the reason for the hairline shear crack observed during the experiment, but did not grow further at the ultimate load.

CHAPTER 8

CONCLUSIONS AND RECOMMENDATIONS

8.1 Conclusions

Beam column joint made with high strength concrete fails by flexure with plastic hinge formation at the interface of the BCJ. This mode of failure is not desirable because yielding of the beam top steel reinforcement can penetrate the core of the BCJ, deteriorates the bond between the steel and concrete and further led to shear failure. It is therefore desirable to relocate the plastic hinge away from the interface of the BCJ to a distance inside the beam.

In new design for code compliant structures, the most suitable way of relocating the plastic hinge away from the BCJ interface is by providing additional reinforcement within the distance of the beam, but this must be done with caution so as not to over-reinforced the section which will change its mode of failure from ductile to brittle.

Externally bonded CFRP is of the most efficient methods for retrofitting existing concrete structures because of its light weight, corrosion resistant, high tensile strength, and ease of application. The conclusions reached after the experimental, numerical and mechanistic studies are as presented below.

- Two and four layers of externally flange bonded CFRP was used to retrofit the original BCJ specimens with adequate development length provided. The plastic hinge was relocated from the interface of the BCJ to the termination length of the CFRP. Two different lengths of CFRP was used; 200mm and 300mm.
- The 200mm length CFRP performed better than 300mm length CFRP in plastic hinge relocation, but the 300mm length CFRP had higher improved section capacity than the 200mm length.

- The retrofitted samples showed increase capacity for both monotonic and reversed cyclic loading tests. The increased capacity ranges from 15%-28%. Higher ductility was also observed in addition to the plastic hinge relocation. The improved section capacity was a result of plastic hinge relocation.
- ABAQUS was used to simulate the test performed experimentally using concrete damage plasticity. The concrete damage plasticity accurately predicts the behavior of the BCJ before and after retrofitting.
- The concrete model used in the ABAQUS model was good enough to predict the behavior of the concrete stress-strain curve during simulation. Although, experimental data are still required for model calibration.
- The Tsai-Wu failure theory used in modelling the CFRP and epoxy in ABAQUS gave a good result when compared with experimental and mechanistic results.

- The master-to-slave technique used in bonding the steel reinforcement to the concrete gives reasonable results, solves convergence problem, and accurately

predict behavior of the steel reinforcement with regards to stress level and yielding strain.

- The analytical equations given in ACI 440 validates the flexural capacity enhancement as observed in the experimental and numerical tests.

8.2 Recommendations

- Behavior of BCJ made with UHPC needs to studied and compared with BCJ made with conventional high strength concrete.

- Effect of concrete grades (above 50MPa) on BCJ needs to be studied which will provide guidelines for professionals in the industry on the need to provide minimum reinforcement at the joint even for low seismic zone.

- Further studies on code compliant BCJ made with high strength concrete need to be conducted, to understand the mode of failure and method of retrofitting such BCJ.

- Further studies can be conducted to determine the effect of CFRP length on the plastic hinge relocation.

- Since the current study only focus on retrofitting, it can be extended for repair of damaged BCJ using externally flange bonded CFRP.

References

[1] Jack Moehle, “Seismic Design of Reinforced Concrete Buildings”. Mc Graw Hill Educational Publisher, 2014.

[2] ACI-ASCE Committee 352, “Recommendations for the design of beam-column connections in monolithic reinforced concrete structures”. (ACI 352R-02), American Concrete Institute, Farmington Hills, MI.,2002.

[3] Saatcioglu, M., Mitchell, D., Tinawi, R., Gardner, N. J., Gillies, A G., Ghobarah A, Anderson, D.L., and Lau, D. “The August 17, 1999, Kocae1i (Turkey) earthquake - damage to structures”. Canadian Journal of Civil Engineering, 2001, 28(4): 715-737.

[4] Uang, C-M., et al., ‘Ji-Ji Taiwan Earthquake of Sep.21, 1999: A Brief Reconnaissance Report’, Department of Structural Engineering, University of California, San Diego, 1999.

[5] Engindeniz, M., “Repair and Strengthening of Pre-1970 Reinforced Concrete Corner Beam-Column Joints Using CFRP Composites”, PhD Thesis, Civil and Environmental Engineering Department, Georgia Institute of Technology, August 2008.

[6] Hassan, W. M., “Analytical and Experimental Assessment of Seismic Vulnerability of Beam-Column Joint without Transverse Reinforcement in Concrete Building”, PhD Thesis, Civil and Environmental Engineering Department, University of California, Berkeley, January 2011.

[7] Hakuto, S., Park, R. and Tanaka, H. “Seismic load tests on interior and exterior beam-column joints with substandard reinforcing details”. ACI Structural Journal, Vol. 97, No. 1, 11-25, 2000.

[8] Le-Trung, Kihak Lee, Jaehong Lee, Do Hyung Lee, and Sungwoo Wooc,” Experimental study of RC beam–column joints strengthened using CFRP composites”, Composites: Part B 41 (2010) 76–85

[9] Eslami A. and Ronagh, H.R., “Experimental Investigation of an appropriate anchorage system for flange-bonded carbon fiber-reinforced polymers in retrofitted RC Beam Column Joints”, ASCE journal of structural engineering, 2013.

[10] Danish Ahmed. “Retrofitting of exterior beam-column joints using CFRP”, a master of science thesis submitted to the department of Civil and Environmental Engineering, King Fahd University of Petroleum and Minerals, Saudi Arabia. 2012.

[11] Franco Shiohara, Kusuhara, “Seismic Retrofit of Reinforced Concrete Beam-Column Joints with CFRP Composites”, University of Tokyo. July 25-29, 2010.

[12] Chris, Chandra and Lawrence, “Rehabilitation of R/C Building Joints with FRP Composites”, University of Utah, 12WCEE 2000.

[13] Ravi Robert et al., "Experimental Investigation on Influence of Development Length in Retrofitting Reinforced Concrete Beam-Column Joints" NBMCW 2009, vol. 4, Pg. 148-158.

[14] Ghobarah Geng, Chajes, Chou & Pan. “The Retrofitting of Reinforced Concrete Column-To-Beam Connections” Composites Science and Technology 58 (1998) 1297-1305.

[15] Sasmal D'Ayala, D., Penford, A., Valentini, S. “Use of FRP fabric for strengthening of Reinforced concrete beam-column joints”. 10th International conference on Structural faults and Repair, London. 2003.

[16] Al-Sayed Tsonos, "Effectiveness of CFRP Jackets and RC Jackets in Post-Earthquake and Pre- Earthquake Retrofitting of Beam Column Sub Assemblages," Journal of Engineering Structures 2008, vol. 30, Pg. 777-793.

[17] Halahla Abdulsamee. “Experimental and Numerical Study for using CFRP for upgrading beam-column joints behavior under cyclic loading,” a PhD thesis submitted to the department of Civil and Environmental Engineering, King Fahd University of Petroleum and Minerals, Saudi Arabia. 2014.

[18] Hadigheh S.A., Maheri M.R., and Mahini S.S. “Performance of weak-beam, strong-column RC frames strengthened at the joints by FRP.” IJST, Transactions of Civil Engineering, vol. 37, No. C1, pp 33-51., 2012.

[19] Hadi, M. N. S. & Tran, T. Minh. Retrofitting nonseismically detailed exterior beam-column joints using concrete covers together with CFRP jacket. Construction and Building Materials, 63, 161-173., 2014.

[20] Wong, H.F., “Shear Strength and Seismic Performance of Non-Seismically Designed Reinforced Concrete Beam-Column Joints”, PhD Dissertation, Department of Civil Engineering, The Hong Kong University of Science and Technology, 2005.

[21] Gogkoz, E., ‘Experimental Research on Seismic Retrofitting of R/C Exterior Beam-Column-Slab Joints Upgraded with CFRP Sheets’, M.Sc. Thesis, Graduate Program in Civil Engineering, Bogaziçi University, 2008.

[22] Barnes, M. and Jigoral, S., “Exterior Non-Ductile Beam Column Joints”. University of California, Berkeley, PEER/NEESREU Research Report, Aug. 2008.

[23] Clyde, C. and Pantelides. 'Performance-Based Evaluation of Exterior Reinforced Concrete Building Joints for Seismic Excitation', University of California, Berkeley, CA, Technical Report PEER 2005-5, Jul. 2000.

[24] Barnes, M. and Jigoral, S., "Exterior Non-Ductile Beam Column Joints". University of California, Berkeley, PEER/NEESREU Research Report, Aug. 2008.

[25] Pantelides, C., Okahashi, Y., and Reaveley, L., "Seismic Rehabilitation of Reinforced Concrete Frame Interior Beam-Column Joints with FRP Composites", Journal of Composites for Construction: (ASCE), 2008.

[26] Karayannis, C. G., Chalioris, C. E., and Sideris, K. K. "Effectiveness of RC beam-column connection repair using epoxy resin injections." Journal of Earthquake Engineering, 2(2), 217-240, 1998.

[27] Antonopoulos, C.P. and Triantafillou, T.C., "Experimental Investigation of FRP Strengthened RC Beam-Column Joints", ACSE J. Compos. Constr., vol. V.7, No. 1, pp.39–49, 2003.

[28] Kim, J., and Oh., G., "Strength deterioration of reinforced concrete beam column joints subjected to cyclic loading", Engineering Structures 31, pp. 2070-2085, 2009.

[29] Bakir, P.G., and Boduroglu, H.M, "A new design equation for predicting the joint shear strength of monotonically loaded exterior beam-column joints". Engineering Structures, vol. No. 24, pp. 1105–1117, 2002.

[30] Vollum RL, 'Design and analysis of exterior beam column connections', PhD thesis, Imperial College of Science Technology and Medicine-University of London, 1998.

[31] Anderson, M., Lehman, D., and Stanton, J., "A Cyclic Shear Stress-Strain Model for Joints without Transverse Reinforcement", Engineering Structures, No. 30, pp.941-954, 2008.

[32] R. Park, "A summary of results of simulated seismic load tests on reinforced concrete beam-column joints, beam and columns with sub-standard reinforcing details", J. Earthquake. Eng., vol. 6, no. 2, pp. 147–174, Apr. 2002

[33] Ilki, Alper, "Behavior of FRP-Retrofitted Joints Built with Plain Bars and Low-Strength Concrete", J. Compos. Constr., vol. 15, no. 3, pp. 312–326, 2011.

[34] Sarsam, K.F., and Phipps, M.E., "The Shear Design of In-situ Reinforced Beam-Column Joints Subjected to Monotonic Loading', Magazine of Concrete Research, vol. 37, no. No. 130, pp. 16–28, 1985.

[35] Sagbas, G. "Nonlinear Finite Element Analysis of Beam-Column Subassemblies", Graduate Department of Civil Engineering University of Toronto, Canada, 2007.

[36] Mitra, N. “Continuum Model for RC Interior Beam-Column Connection Regions” presented at the 14th World Conference on Earthquake Engineering, Beijing, China, 2008.

[37] Dassault Systems. “Abaqus Overview, Abaqus Unified FEA. Retrieved July 29, 2015, from http://www.3ds.com/products-services/simulia/portfolio/abaqus/2015.

[38] Mahini, S. S. and Ronagh, H. R., “Strength and ductility of FRP web-bonded RC beams for the assessment of retrofitted beam–column joints”, Composite Structures, 92(6), 1325-32, 2010.

[39] ACI Committee 440.2. “Guide for the design and construction of externally bonded FRP systems for strengthening concrete structures (ACI 440.2R-02)”, American Concrete Institute, Farmington Hills, MI., 2002.

[40] ACI Committee 318. Building code requirements for structural concrete (ACI 318-14) and commentary (318R-14), American Concrete Institute, Farmington Hills, MI., 2015.

[41] Teng, J.G., Lu, X.Z., Ye, L.P., and Jiang, J.J. “Recent research on intermediate crack induced debonding in FRP strengthened beams”. Proceedings of the 4th international conference on advanced composite materials for bridges and structures, Calgary, AB, Canada, 2004.

[42] ASTM C39/C39M-04a, “Standard Test Method for Compressive Strength of Cylindrical Concrete Specimens”, 2004.

[43] ASTM C 496/C 496M - 04, “Standard Test Method for Splitting Tensile Strength of Concrete Specimens”, 2004.

[44] ASTM C469-94, “Standard Test Method for Static Modulus of Elasticity and Poisson’s Ratio of Concrete in Compression”, 1994.

[45] ASTM A615/A615M, “Standard Specification for Deformed and Plain Carbon-Steel Bars for Concrete Reinforcement”, 2016.

[46] Tsonos, A. G. “Effectiveness of CFRP-jackets and RC-jacket in post-earthquake and pre-earthquake retrofitting of beam-column sub assemblages”. Eng Struct; 30: 640 777-93, 2007.

Vitae

Name	:Olaniyi Solomon Arowojolu
Nationality	:Nigerian
Date of Birth	:3/30/1988
Email	:olaniyiarowojolu@gmail.com
Address	:27, Bisi Adelesi Street, Agiliti, Lagos, Nigeria
Academic Background	: M.Sc. Civil Engineering, November, 2016 King Fahd University of Petroleum and Minerals, Saudi Arabia. B.Sc. Civil & Environmental Engineering, December, 2010 University of Lagos, Akoka. Nigeria.
Presentation/Publications:	Baluch M.H and **Olaniyi S.A**, "A new trend in Concrete Research" Joint ACI-SIKA seminar, Al-Khobar, Saudi Arabia, 2016. M.K. Rahman, **O.S. Arowojolu**, M.H. Baluch, A.H. Gadhib and M.A Osta. "Relocating the plastic hinge at the beam column joint interface into the beam in CFRP strengthening." CICE., December, 2016.